

hep-th/9807170
RU-98-27

Calabi-Yau Spaces and Five Dimensional Field Theories with Exceptional Gauge Symmetry

Duiliu-Emanuel Diaconescu and Rami Entin

Department of Physics and Astronomy

Rutgers University

Piscataway, NJ 08855-0849

duiliu, rami@physics.rutgers.edu

Five dimensional field theories with exceptional gauge groups are engineered from degenerations of Calabi-Yau threefolds. The structure of the Coulomb branch is analyzed in terms of relative Kähler cones. For low number of flavors, the geometric construction leads to new five dimensional fixed points.

1. Introduction and Summary

Five dimensional gauge theories with $\mathcal{N} = 1$ supersymmetry are in general not renormalizable and therefore should be viewed as theories with a cut-off. An exception to this occurs if a theory is defined by an interacting UV fixed point of the renormalization group. Concrete examples with one dimensional Coulomb branch have been discovered for the first time in [1] by studying D4-branes near orientifold fixed planes. The same theories are associated to del Pezzo contractions in Calabi-Yau threefolds in [2,3].

Theories with higher rank gauge groups and their corresponding Calabi-Yau degenerations were considered in [4,5]. The exact quantum prepotential for general gauge groups and matter content was determined, and complete list of possible fixed points with a gauge theory origin was given. A necessary condition for the existence of a fixed point is that the metric on the Coulomb branch will be non-negative which gives an upper bound on the allowed number of matter representations. Alternatively, one can use Higgsing arguments to limit the number of flavors in the higher rank theory if the bound in the lower rank theory is known. The precise agreement found between the gauge theory calculation of the prepotential and its geometric counterpart allows one to address the issue of existence of fixed points directly in the geometry. In some cases it is possible to determine that a necessary condition is also sufficient. This was done by [4] for certain classical groups with restricted matter representations. An alternative approach based on brane constructions appeared in [6,7]. As shown in [8] all the theories that arise this way can also be realized by compactifying M-theory on torically degenerated Calabi-Yau spaces.

The subject of the present paper is exceptional gauge group theories with matter content in the smallest allowed representations. As in [4] we find a complete agreement between the gauge theory prepotential and the one computed from triple intersections of the corresponding Calabi-Yau degeneration. Our main result concerns the existence of fixed points. We perform in detail the geometric analysis and show that some of the necessary conditions found in [4] are also sufficient. Concretely, we show the existence of the following fixed point theories

$$\begin{aligned}
 G_2 \quad & n_7 \leq 4 \\
 F_4 \quad & n_{26} \leq 3 \\
 E_8 \quad & n_{248} = 0 . \\
 E_6 \quad & n_{27} \leq 3 \\
 E_7 \quad & n_{\frac{1}{2}56} \leq 5
 \end{aligned} \tag{1.1}$$

The Coulomb branches of the E_6 and E_7 theories turn out to have an interesting phase structure already in the presence of massless matter. Finally, as expected by the absence of a certain global anomaly in the E_7 gauge theory, we find that theories with an odd number of half **56** hypermultiplets do occur.

The plan of this paper is as follows. In the rest of this section we give a short summary of the properties of five dimensional gauge theories we will need and briefly review the geometry-gauge theory correspondence. The relatively simple cases of G_2 , F_4 and E_8 gauge theories are discussed in section 2. Sections 3 and 4 are devoted to the E_6 and E_7 theories respectively. Appendix A contains a summary of the relevant facts about ruled surfaces. The canonical resolutions of the E_6 and E_7 singularities which are the starting points of constructing the corresponding Calabi-Yau degenerations are given in appendices B and C.

1.1. Five dimensional gauge theories

Following [1,2,4], we recall some relevant features of five dimensional gauge theories. Along the Coulomb branch, the effective low energy description of a theory with an exceptional gauge group G of rank r is that of an Abelian gauge theory with r $U(1)$ gauge fields. It is determined in terms of the prepotential $\mathcal{F}(\phi^i)$ where ϕ^i are the scalar partner of the r $U(1)$ vectors. Five dimensional gauge invariance constrains $\partial_i \partial_j \partial_k \mathcal{F}$ to be integral which restricts the local form of the prepotential to be at most cubic in ϕ^i . Therefore the exact quantum prepotential is determined already at one-loop. For massless matter in representations \mathbf{r}_f of G , it is given by¹

$$\mathcal{F} = \frac{1}{2} m_0 h_{ij} \phi^i \phi^j + \frac{1}{12} \left(\sum_{\mathbf{r} \in \mathbf{R}} |\mathbf{r} \cdot \phi|^3 - \sum_f \sum_{\mathbf{w} \in \mathbf{W}_f} |\mathbf{w} \cdot \phi|^3 \right), \quad (1.2)$$

where h_{ij} is the trace $\text{Tr } T_i T_j$ of the Cartan generators, and \mathbf{R} and \mathbf{W}_f are the weight systems of the adjoint and matter representations. The first two terms are present at the classical level. The last two are generated quantum mechanically by integrating out massive gauge bosons and charged matter which contribute with opposite signs to the prepotential.

¹ We consider exceptional gauge groups whose d symbol vanishes, making a classical Chern-Simons term impossible.

The signs of the $\mathbf{r} \cdot \phi$ terms are identical for all $\mathbf{r} \in \mathbf{R}$ in any given Weyl chamber. Choosing a definite sign for the first quantum term in (1.2) gives an expression which is valid throughout the Weyl chamber. A non-trivial phase structure emerges when $\mathbf{w} \cdot \phi$ vanishes along certain codimension one boundaries inside the Weyl chamber, creating a wedge structure. Since these terms enter the prepotential with an absolute value there are different prepotentials in each of the sub-wedges. The metric on the Coulomb branch is still continuous since it is determined by the Hessian $g_{ij} = \partial_i \partial_j \mathcal{F}$.

As mentioned earlier, a necessary condition for the existence of fixed point is that the metric should be non-negative on the entire Coulomb branch. Only then it is possible to have a sensible quantum theory on the entire moduli space, since a breakdown of the metric is a sign of non-renormalizability. This condition is equivalently expressed as the requirement that \mathcal{F} be a convex function on the entire Weyl chamber. The gauge bosons term is obviously convex since it enters the prepotential with a positive sign. The negative sign of the matter contribution makes that term concave. Thus, a necessary condition for the existence of fixed points will be in the form of an upper bound on the number of flavors.

1.2. Gauge theory from geometry

Here we review the basic ideas of geometric engineering [9,10,11,12] following closely [4]. Non-Abelian gauge theories in five dimensions arise from compactifications of M-theory on singular Calabi-Yau manifolds. The singularity structure is studied in terms of the resolved space $\pi : X \rightarrow \bar{X}$ which contains a collection of rationally ruled surfaces S_j shrinking to a curve \bar{C} in \bar{X} . Under the map π the holomorphic curve class $[\epsilon_j]$ of the ruling on each surface shrinks to a point in \bar{C} . Membranes wrapping the generic fibers yield BPS states filling out a non-Abelian vector multiplet. More precisely, the simple roots of G are identified with the divisor classes $[S_i] \in H^2(X, \mathbf{Z})$ and the generic fibers $[\epsilon_j] \in H_2(X, \mathbf{Z})$ with the simple co-roots. Their intersection form reproduces the Cartan matrix of G ²:

$$S_i \cdot \epsilon_j = -C_{ij}. \quad (1.3)$$

For simply laced groups, all divisors are ruled over curves of the same genus g which determines the number of hypermultiplets [13]. In the non-simply laced case, the divisors

² We do not differentiate in the text between the Cartan matrix its minus. The correct signs appear in the formulas.

corresponding to short simple roots intersect those corresponding to long roots along double or triple sections of genus g' . The genus g of a simple section determines the number of adjoint hypermultiplets. As explained below, we also obtain $g' - g$ extra hypermultiplets in a different representation.

There are two distinct deformations corresponding to charged matter. The first, generically associated to simply laced groups³, consists of blowing-up a given number of points on the minimal rulings. The resulting exceptional curves σ_k account for weight vectors of certain group representations. More precisely, $H_2(X, \mathbf{Z})$ is identified with the weight lattice of G . The intersection numbers of the holomorphic curves σ_k with the exceptional divisors S_i reproduce the weight system of the matter representation. All the other weight vectors are obtained by adding linear combinations of the generic fiber classes to σ_k . The number of flavors is controlled by the number of independent exceptional curves, or in some cases, the number of configurations of exceptional curves.

The second deformation is characteristic to non-simply laced groups when one of the simple co-roots is already a weight of a matter representation other than the adjoint. The low energy theory then contains $g' - g$ charged hypermultiplets. Note that in this case, a non-trivial matter content can be engineered with minimally ruled surfaces. The **7** representation of G_2 and the **26** representation of F_4 are included in this category.

Since the area of the curve \bar{C} is inversely proportional to the classical gauge coupling, a necessary and sufficient condition for the existence of a fixed point is the existence of a contraction, mapping \bar{C} to a point. As shown in [4], this condition implies that the prepotential is convex. A sufficient condition for the existence of this contraction map is that the restriction to each surface S_j of a generic class in the relative Kähler cone $\mathcal{K}(X/\bar{X})$ is ample. Thus, one has to check that these restrictions have positive intersection numbers with all irreducible holomorphic curves on each S_j . We show that this condition is satisfied if the number of flavors is low enough, thus establishing the existence of fixed point theories.

2. G_2 , F_4 and E_8

As stated in the introduction, we begin the analysis with the simple cases which can be realized in terms of minimally ruled surfaces. This is a known feature of non-simply laced groups noted in [4]. E_8 is included in the same category since the smallest matter representation is also the adjoint.

³ Note that there is an exception to this rule, namely $Sp(N)$ gauge groups and fundamental representation.

2.1. G_2 with n_7 quarks

Since G_2 has rank two, the corresponding degeneration consists of two rationally ruled surfaces S_1, S_2 over curves γ_1, γ_2 where γ_1 is a triple cover of γ_2 . In order to avoid generation of adjoint matter, γ_1 is taken of genus zero while the genus of γ_2 determines the number of fundamental quarks $g = n_7$.

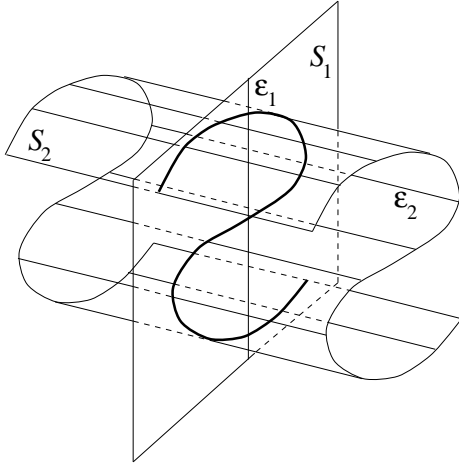


Fig. 1: G_2 degeneration

Let $\epsilon_{1,2}$ denote the fiber classes of the rulings. The intersection matrix of the degeneration is the G_2 Cartan matrix

$$\epsilon_i \cdot S_j = \begin{bmatrix} -2 & 3 \\ 1 & -2 \end{bmatrix}. \quad (2.1)$$

The matter content can be easily derived noting that the fiber class ϵ_2 is actually a weight vector for the **7** representation. The other weight vectors can be realized as linear combinations of $\epsilon_{1,2}$. An arbitrary divisor supported on the exceptional locus can be written as

$$S = \phi_1 S_1 + \phi_2 S_2 \quad (2.2)$$

where $\phi_{1,2}$ are coordinates on the negative relative Kähler cone of the degeneration $-\mathcal{K}(X/\bar{X})$. The latter is defined by

$$-S \cdot \epsilon_i > 0, \quad i = 1, 2, \quad (2.3)$$

therefore it corresponds to the fundamental Weyl chamber of G_2 . The prepotential is given by the triple intersection

$$\mathcal{F} = \frac{1}{6} S^3. \quad (2.4)$$

Since the two surfaces intersect along a curve of genus g in the Calabi-Yau space, we have

$$S_1^2 S_2 + S_1 S_2^2 = 2g - 2. \quad (2.5)$$

As γ is a 3-section in S_1 , $\gamma = 3C^\infty + a\epsilon_1$ and the adjunction formula shows that

$$(\gamma^2)_{S_1} = 3(g + 2). \quad (2.6)$$

Therefore

$$S_1 S_2^2 = 3(g + 2), \quad S_1^2 S_2 = -g - 8 \quad (2.7)$$

and S_1, S_2 are ruled surfaces of degrees $n_1 = \frac{1}{3}(g + 2(1 - a))$ $n_2 = g + 8$. The final formula for the prepotential is

$$\mathcal{F} = 8\phi_1^3 + 8(1 - g)\phi_2^3 + 9(g + 2)\phi_1\phi_2^2 - 3(g + 8)\phi_1^2\phi_2 \quad (2.8)$$

which agrees with the gauge theory computation. Note that the result does not depend on the multiplicity a of the fiber in the 3-section γ . However, this will turn out to be important for the existence of fixed points. In principle, a can be taken zero unless a non-zero value is required by the integrality of n_1 and g . In the present cases, we consider fixed values of a as follows

$$a = \begin{cases} 1, & g \equiv 0 \pmod{3} \\ 0, & g \equiv 1 \pmod{3} \\ 2, & g \equiv 2 \pmod{3} \end{cases} \quad (2.9)$$

This implies that $n_1 \geq 0$.

Next, we address the issue of the existence of UV fixed points. In order to apply the method of [4] based on contraction criteria we need to explicitly find the extremal rays of the Kähler cone (2.3). This can be done systematically noting that the inequalities (2.3) can be rewritten in the form

$$a_i > 0, \quad i = 1, 2 \quad (2.10)$$

by a linear change of variables

$$a_i = C_{ij}\phi_j. \quad (2.11)$$

Therefore the divisors on the extremal rays are determined by the columns of the G_2 quadratic form⁴

$$L_i = \sum_j (C^{-1})_{ij} S_j. \quad (2.12)$$

⁴ Strictly speaking, $(C^{-1})_{ij}$ is the G_2 quadratic form with the second column multiplied by 3. In the inequalities we consider this difference is not important.

Concretely,

$$L_1 = 2S_1 + S_2, \quad L_2 = 3S_1 + 2S_2. \quad (2.13)$$

Note that this procedure of determining the extremal rays is general and will be applied for all cases studied in this paper. In certain situations, the resulting cone is divided into sub-cones corresponding to different geometric phases. This complication does not arise for minimally ruled configurations.

Following the strategy adopted in [4], we now check that the divisors L_i lying on the extremal rays contract certain S_j and induce ample classes on the resulting birational models. We have

$$\begin{aligned} -L_1 \cdot S_1 &= C_1^\infty + \left(\frac{a}{3} + \frac{2}{3}(4-g) \right) \epsilon_1 \\ -L_1 \cdot S_2 &= (g+10)\epsilon_2 \\ -L_2 \cdot S_1 &= (4-g)\epsilon_1 \\ -L_2 \cdot S_2 &= C_2^\infty + (g+12)\epsilon_2. \end{aligned} \quad (2.14)$$

It follows that L_1 contracts S_2 along the ruling and it restricts to an ample divisor on S_1 if $g < 4$. If $g = 4$, L_1 intersects $S_1 \simeq \mathbf{F}_2$ along C_1^∞ . Therefore it also contracts C_1^0 yielding the cone \bar{S}_1 on which C_1^∞ is ample. Similarly, L_2 contracts S_1 along the ruling if $g < 4$ and it is ample on \bar{S}_2 . If $g = 4$, L_2 contracts S_1 and the zero section on S_2 yielding the cone \bar{S}_2 . Therefore, the class $-L_2 \cdot S_2$ is ample on \bar{S}_2 . We conclude that the theories exhibit UV fixed points for $g \leq 4$. This is precisely the necessary condition derived in [4] based on Higgsing arguments. The above analysis proves that it is also sufficient.

2.2. F_4 with n_{26} quarks

The degeneration consists of a chain of four rationally ruled surfaces S_1, \dots, S_4 intersecting along common curves $\gamma_1, \dots, \gamma_3$ as in fig. 2. S_1 and S_2 are ruled over rational curves while S_3 and S_4 are ruled over curves of genus $g = n_{27}$. The curve $\gamma_2 = S_2 \cap S_3$ covers the rational base of S_2 twice.

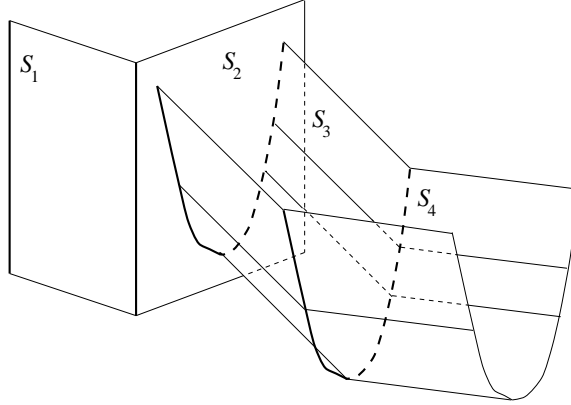


Fig. 2: F_4 degeneration

The intersection matrix

$$\epsilon_i \cdot S_j = \begin{bmatrix} -2 & 1 & 0 & 0 \\ 1 & -2 & 2 & 0 \\ 0 & 1 & -2 & 1 \\ 0 & 0 & 1 & -2 \end{bmatrix}. \quad (2.15)$$

reproduces correctly the F_4 Cartan matrix. The matter content can be easily determined by noting that all the weight vectors of **26** can be written as linear combinations of the fiber classes $\epsilon_1, \dots, \epsilon_4$. The relative Kähler cone of the degeneration is defined by

$$-S \cdot \epsilon_i > 0, \quad i = 1, \dots, 4 \quad (2.16)$$

where $S = \sum_{i=1}^4 \phi_i S_i$ is an arbitrary divisor supported on the exceptional locus. These conditions define again the fundamental Weyl chamber as expected from gauge theory considerations. In order to compute the prepotential (2.4), we have to evaluate all triple intersections of the form $S_i \cdot S_j \cdot S_k$. Since γ_2 is a 2-section of S_2 , the adjunction formula yields

$$(\gamma_2)^2 = 4(g+1), \quad n_2 = g+1. \quad (2.17)$$

Using (2.5), it follows that

$$\begin{aligned} S_1^2 S_2 &= -g-1, & S_1 S_2^2 &= g-1 \\ S_2^2 S_3 &= -2g-6, & S_2 S_3^2 &= 4(g+1) \\ S_3^2 S_4 &= -8, & S_3 S_4^2 &= 2g+6. \end{aligned} \quad (2.18)$$

Note that these relations determine the degrees of the ruled surfaces S_1, \dots, S_4

$$\begin{aligned} n_1 &= g - 1 & n_3 &= 2g + 6 \\ n_2 &= g + 1 & n_4 &= 8. \end{aligned} \tag{2.19}$$

Therefore the prepotential is given by

$$\begin{aligned} \mathcal{F} = & 8\phi_1^3 - 3(g+1)\phi_1^2\phi_2 + 3(g-1)\phi_1\phi_2^2 + 8\phi_2^3 + 12(g+1)\phi_2\phi_3^2 - 3(2g+6)\phi_2^2\phi_3 \\ & + 8(1-g)\phi_3^3 + 3(2g+6)\phi_3\phi_4^2 - 24\phi_3^2\phi_4 + 8(1-g)\phi_4^3. \end{aligned} \tag{2.20}$$

It can be checked by direct computation that this agrees with the one loop prepotential in gauge theory.

According to the general procedure outlined above, the fixed point conditions can be expressed in terms of divisors L_i , $i = 1, \dots, 4$ lying on the extremal rays of the relative Kähler cone. These can be read off directly from the F_4 quadratic form as in (2.12). Next, we check that L_i either contract certain S_j or induce ample classes on the resulting birational models. Consider for example,

$$L_1 = 2S_1 + 3S_2 + 2S_3 + S_4. \tag{2.21}$$

We have

$$\begin{aligned} -L_1 \cdot S_1 &= C_1^\infty + 2(3-g)\epsilon_1 \\ -L_1 \cdot S_2 &= (5-g)\epsilon_2 \\ -L_1 \cdot S_3 &= 2(5-g)\epsilon_3 \\ -L_1 \cdot S_4 &= 2(5-g)\epsilon_4. \end{aligned} \tag{2.22}$$

This shows that L_1 contracts S_2, S_3 and S_4 along the ruling and reduces to an ample divisor on S_1 if $g < 3$. If $g = 3$, L_1 also contracts the zero section on S_1 and the induced class is ample on the resulting cone \bar{S}_1 . The divisors corresponding to the remaining rays can be treated similarly. We conclude that a sufficient condition for the existence of fixed points with F_4 gauge symmetry is $n_{26} \leq 3$. Note that this is again precisely the necessary condition derived from a Higgsing argument in [4].

2.3. E_8 with n_{248} quarks

Since the matter multiplets transform in the adjoint representation, the degeneration consists of a chain of rationally ruled surfaces intersecting along sections according the E_8 Dynkin diagram. There are no multiple covers since E_8 is simply laced. The number of adjoint quarks is equal to the genus of the common base. Such a configuration results naturally from the resolution of a curve of E_8 singularities in the Calabi-Yau manifold.

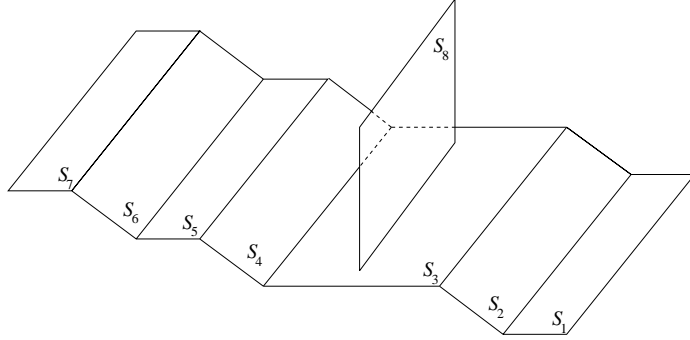


Fig. 3: E_8 degeneration

It is straightforward to check that the intersection matrix $\epsilon_i \cdot S_j$ reproduces the E_8 Cartan matrix. The superpotential is given again by the triple intersection (2.4). The intersection numbers $S_i \cdot S_j \cdot S_k$ can be computed starting from S_3 . This minimally ruled surface must have three disjoint sections corresponding to the intersections with S_2, S_4, S_8 . The only way this can be realized is if S_3 is a surface of degree zero, therefore

$$S_3 S_2^2 = S_3 S_4^2 = S_3 S_8^2 = 0. \quad (2.23)$$

The remaining intersection numbers can be computed recursively

$$\begin{aligned} S_2 S_3^2 &= S_4 S_3^2 = S_8 S_3^2 = 2g - 2 \\ S_1^2 S_2 &= S_4 S_5^2 = 2 - 2g \\ S_1 S_2^2 &= S_4^2 S_5 = 4g - 4 \\ S_5 S_6^2 &= 4 - 4g, \quad S_5^2 S_6 = 6g - 6 \\ S_6 S_7^2 &= 6 - 6g, \quad S_6^2 S_7 = 8g - 8. \end{aligned} \quad (2.24)$$

The degrees of the rulings turn out to be

$$\begin{aligned} n_1 &= n_5 = 4g - 4 & n_6 &= 6g - 6 \\ n_2 &= n_4 = n_8 = 2g - 2 & n_7 &= 8g - 8. \\ n_3 &= 0 \end{aligned} \quad (2.25)$$

The prepotential resulting from (2.24) is given by

$$\begin{aligned} \mathcal{F} = & 8\phi_1^3 + 18\phi_1^2\phi_2 - 24\phi_1\phi_2^2 + 8\phi_2^3 + 12\phi_2^2\phi_3 - 18\phi_2\phi_3^2 + 8\phi_3^3 + 6\phi_3^2\phi_4 - 12\phi_3\phi_4^2 \\ & + 8\phi_4^3 - 6\phi_4\phi_5^2 + 8\phi_5^3 - 6\phi_5^2\phi_6 + 8\phi_6^3 - 12\phi_6^2\phi_7 + 6\phi_6\phi_7^2 + 8\phi_7^3 - 6\phi_5\phi_8 + 8\phi_8^3 \end{aligned} \quad (2.26)$$

and agrees with the gauge theory computation.

The fixed point analysis follows the same steps as in the previous examples. Since there are no subtle points, we do not present the details here. The result is that the divisors corresponding to extremal rays contract most of the surfaces along a ruling or reduce to ample classes on birational models if $g \leq 1$. The case $g = 1$ is special as it corresponds to an $N = 4$ gauge theory. Geometrically, the Calabi-Yau threefold reduces to a direct product $T^2 \times K3$. It is known that these theories cannot exhibit superconformal fixed points [14]. Therefore, there is a unique fixed point with E_8 gauge symmetry corresponding to the theory without matter.

3. E_6 with n_{27} quarks

3.1. Degenerations and phase structure

A systematic procedure for constructing E_6 degenerations with matter is to start from an F-theory compactification on a singular Weierstrass model. The type of singular elliptic fibers and the associated matter content have been classified in [15,16]. The strategy is to construct a smooth elliptic model as in [17,18,19,20]. Finally, we can take the M-theory limit by sending the size of the original elliptic fiber to infinity. We explicitly carry out this procedure for E_6 in appendix B. The result is presented in the figure below.

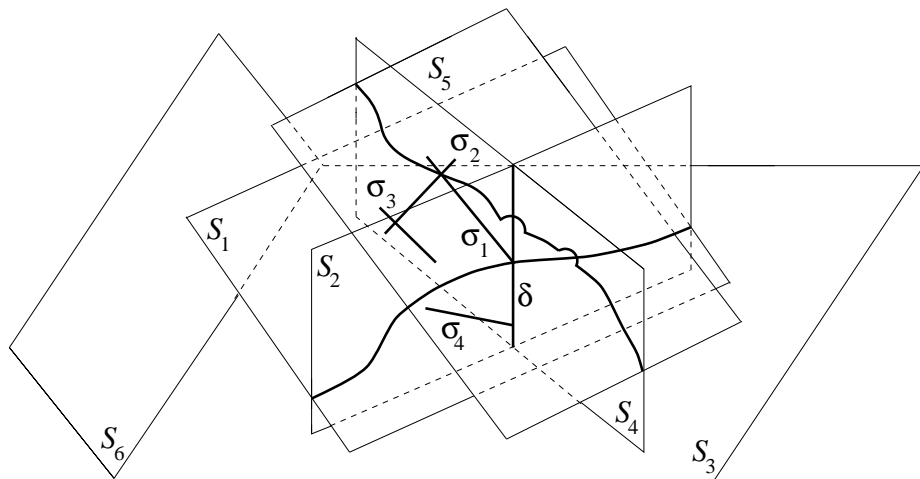


Fig. 4: E_6 degeneration - phase I

The surfaces S_2, S_3, S_5 and S_6 are minimally ruled, while the surfaces S_1, S_4 are blown-up twice so that they each contain a reducible fiber with three components

$$\begin{aligned}\epsilon_1 &= \sigma_1 + \sigma_2 + \sigma_3, \\ \epsilon_4 &= \sigma_1 + \delta + \sigma_4.\end{aligned}\tag{3.1}$$

All surfaces are ruled over rational curves. Note that S_2 and S_4 intersect along the curve δ which is a fiber of S_2 and a (-2) curve on S_4 . Similarly, S_1 and S_5 intersect along σ_2 which is a fiber in the ruling of S_5 and a (-2) curve on S_1 . S_1 and S_4 intersect along σ_1 which is an exceptional (-1) curve in both surfaces. Next, S_5 intersects S_4 along a section passing through the (-1) curve σ_1 and S_2 intersects S_1 along a similar section. The intersection matrix of $\sigma_1, \dots, \sigma_4$ and δ with the exceptional divisors is given by

	S_1	S_2	S_3	S_4	S_5
σ_1	-1	1	0	-1	1
σ_2	0	0	0	1	-2
σ_3	-1	0	0	0	1
σ_4	0	1	0	-1	0
δ	1	-2	1	0	0

(3.2)

It can be easily checked that (3.1) and (3.2) reproduce the E_6 Cartan matrix. Note also that $\sigma_1, -\sigma_3$ and $-\sigma_4$ are weight vectors of the **27** representation. The other weights can be written as linear combinations of $\sigma_{1,3,4}$ and the fiber classes. The relative Kähler cone corresponding to the present degeneration is determined by

$$\begin{aligned}-S \cdot \epsilon_i &> 0, \\ -S \cdot \sigma_k &> 0, \quad -S \cdot \delta > 0\end{aligned}\tag{3.3}$$

where $D = \sum_{i=1}^6 \phi_i S_i$. To make the fixed point analysis later on easier, it is more convenient to work in the coordinates

$$a_i = C_{ij} \phi_j, \tag{3.4}$$

where the external cone determined by the first set of inequalities is the positive 'quadrant' $a_i > 0$. The $\sigma_{3,4}$ inequalities define a sub-cone⁵ which is the intersection of the cones

$$\begin{aligned}\phi_5 &< \phi_1, \\ \phi_2 &< \phi_4\end{aligned}\tag{3.5}$$

⁵ Note that the σ_1 inequality is redundant.

with the first quadrant. We call the phase corresponding to this sub-cone phase I. The form of the inequalities (3.5) in the a_i coordinates can easily be read off by taking the corresponding rows of the E_6 quadratic form

$$\begin{aligned} 2a_1 + a_2 - a_4 - 2a_5 &> 0, \\ 2a_4 + a_5 - a_1 - 2a_2 &> 0. \end{aligned} \tag{3.6}$$

The guiding principle for uncovering the rest of the phases is finding the degenerations which invert the inequalities (3.5). Flopping the exceptional curves σ_k from one surface to another changes their intersection matrix with the divisors S_i . This leads to new inequalities which further subdivide the relative Kähler cone and hence give rise to additional phases. As a consistency check one has to verify that all phases are mutually disjoint and that their union is exactly the extended Kähler cone determined by the first inequalities in (3.3).

On the boundaries of the different sub-wedges charged hypermultiplets are going to zero mass. This means that even though the order by which we proceed to invert the inequalities (3.5) is not unique, the phase structure that we find is. Indeed, in some cases it is very difficult to see in the geometry the flops relating one degeneration to another one. However, by checking the consistency of this scheme as outlined above, we can be reasonably sure that the phase structure we describe is the correct one.

Phase II - The diagram describing this degeneration is identical to fig. 4, but with σ_3 flopped from S_1 to S_5 . It follows that the reducible fibers are now given by

$$\begin{aligned} \epsilon_1 &= \sigma_1 + \sigma_2 \\ \epsilon_4 &= \sigma_1 + \delta + \sigma_4 \\ \epsilon_5 &= \sigma_2 + \sigma_3. \end{aligned} \tag{3.7}$$

The intersection matrix with the exceptional divisors is given by

	S_1	S_2	S_3	S_4	S_5
σ_1	-1	1	0	-1	1
σ_2	1	0	0	1	-1
σ_3	1	0	0	0	-1
σ_4	0	1	0	-1	0
δ	1	-2	1	0	0

As before, and in all other phases below, this intersection matrix correctly reproduces the Cartan matrix and the curves which are not simple co-roots are weight vectors of the **27** representation. The inequalities which define this phase can be read off from (3.8):

$$\begin{aligned} \phi_1 &< \phi_5 \\ \phi_2 &< \phi_4 \\ \phi_4 &< \phi_1 + \phi_5 \\ \phi_2 + \phi_5 &< \phi_1 + \phi_4. \end{aligned} \tag{3.9}$$

Note that the σ_1 inequality is no longer redundant and will therefore have to be inverted.

Phase III - The degeneration corresponding to this phase is described in fig. 5 below.

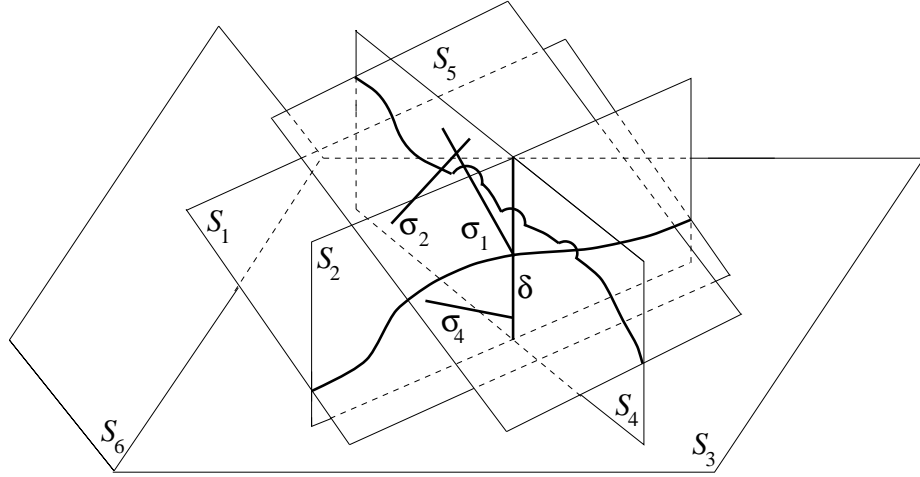


Fig. 5: E_6 degeneration - phase III

All the surfaces are ruled over rational curves and for S_4 the ruling is minimal. The S_4 fiber has four components and is given

$$\epsilon_4 = \sigma_1 + \delta_4 + \sigma_4 + \sigma_2. \tag{3.10}$$

S_1 and S_4 intersect along σ_1 which is the fiber in the ruling of S_1 . S_2 and S_4 intersect along δ which is the fiber in the ruling of S_2 . The section of S_4 along which it intersects S_5 passes through σ_2 and avoids δ and σ_1 . The intersection matrix of these curves with the surfaces S_j is therefore given by

	S_1	S_2	S_3	S_4	S_5
σ_1	-2	1	0	0	0
σ_2	1	0	0	-1	1
σ_4	0	1	0	-1	0
δ	1	-2	1	0	0

, (3.11)

leading to the following inequalities defining phase III

$$\begin{aligned}\phi_2 &< \phi_4 \\ \phi_1 + \phi_5 &< \phi_4.\end{aligned}\tag{3.12}$$

The inequalities above imply

$$\begin{aligned}\phi_1 &< \phi_5 \\ \phi_2 + \phi_5 &< \phi_1 + \phi_4,\end{aligned}\tag{3.13}$$

where the first one follows from the second inequality in (3.12) by using the ϵ_5 inequality in (3.3) and the second follows again from the second inequality in (3.12) by adding ϕ_1 to both sides and using the ϵ_1 inequality in (3.3). This shows that phase III is disjoint from phase I.

Phase IV - The degeneration corresponding to this phase is identical to that described in fig. 4 except that σ_2 is flopped from S_4 to S_2 . The non-minimally ruled surfaces are S_1, S_2 and S_4 whose reducible fibers are given by

$$\begin{aligned}\epsilon_1 &= \sigma_1 + \sigma_2 + \sigma_3 \\ \epsilon_2 &= \delta + \sigma_4 \\ \epsilon_4 &= \delta + \sigma_1.\end{aligned}\tag{3.14}$$

The intersection matrix is given by

$$\begin{array}{c|ccccc} & S_1 & S_2 & S_3 & S_4 & S_5 \\ \hline \sigma_1 & -1 & 1 & 0 & -1 & 1 \\ \sigma_2 & 0 & 0 & 0 & 1 & -2 \\ \sigma_3 & -1 & 0 & 0 & 0 & 1 \\ \sigma_4 & 0 & -1 & 0 & 1 & 0 \\ \hline \delta & 1 & -1 & 1 & -1 & 0 \end{array},\tag{3.15}$$

leading to the inequalities

$$\begin{aligned}\phi_5 &< \phi_1 \\ \phi_4 &< \phi_2 \\ \phi_2 + \phi_5 &< \phi_1 + \phi_4 \\ \phi_1 + \phi_3 &< \phi_2 + \phi_4.\end{aligned}\tag{3.16}$$

It is clear that this phase is disjoint from all the previous ones.

Phase V - The present degeneration is described in fig. 6 below.

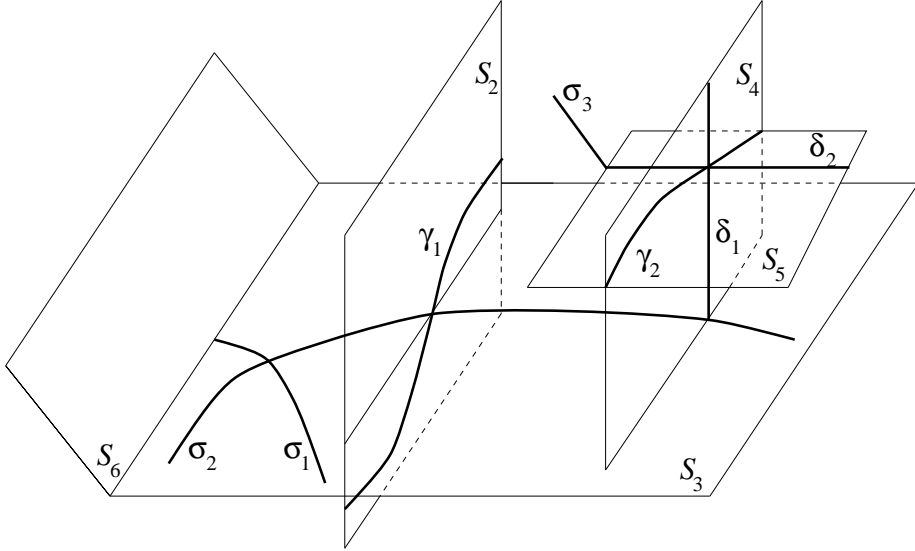


Fig. 6: E_6 degeneration - phase V

The non-minimally ruled surfaces are S_3 and S_1 which intersects S_2 along γ_1 . This surface is too complicated to draw, but we encourage the reader to use her or his imagination. The irreducible fibers are given by

$$\begin{aligned}\epsilon_1 &= \sigma_2 + \delta_1 + \delta_2 + \sigma_3 \\ \epsilon_3 &= \sigma_1 + \sigma_2.\end{aligned}\tag{3.17}$$

The intersection matrix is given by

	S_1	S_2	S_3	S_4	S_5	S_6	
σ_1	1	0	-1	0	0	1	
σ_2	-1	1	-1	1	0	0	
σ_3	-1	0	0	0	1	0	
δ_1	0	0	1	-2	-1	0	
δ_2	0	0	0	0	1	-2	

The inequalities defining this phase are therefore

$$\begin{aligned}\phi_2 + \phi_4 &< \phi_1 + \phi_3 \\ \phi_5 &< \phi_1 \\ \phi_1 + \phi_6 &< \phi_3.\end{aligned}\tag{3.19}$$

It is straight forward to verify that these imply

$$\begin{aligned}\phi_4 &< \phi_2 \\ \phi_2 + \phi_5 &< \phi_1 + \phi_4,\end{aligned}\tag{3.20}$$

which shows that this phase is disjoint from phases I, II and III. By the first inequality in (3.19), it is manifestly disjoint from phase IV as well.

Phases VI and VII - These are obtained by flopping σ_1 , first from S_3 to S_6 and then outside S_6 as described in the figure 7 below.

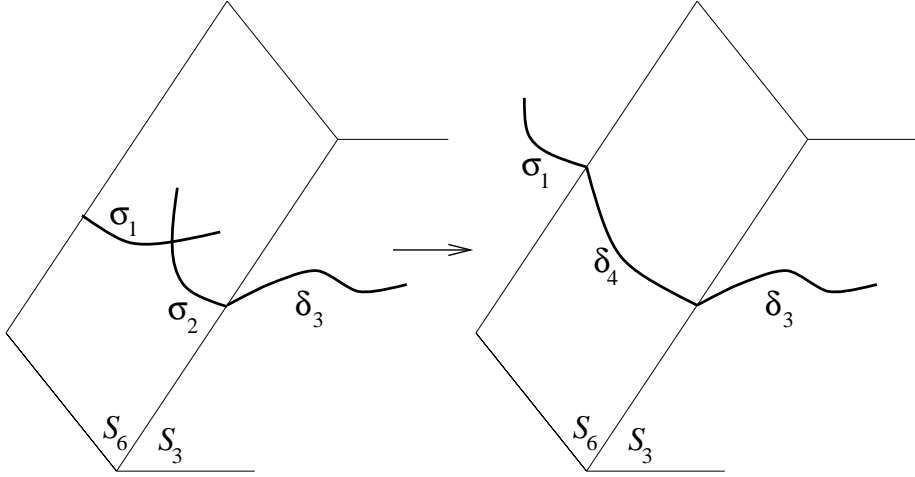


Fig. 7: E_6 degeneration - phases VI and VII

The changes from the degeneration corresponding to phase V are

	phase VI	phase VII	
ϵ_1	$\sigma_3 + \delta_1 + \delta_2$ + $\delta_3 + \sigma_1$	$\sigma_3 + \delta_1 + \delta_2$ + $\delta_3 + \delta_4 + \sigma_1$	
ϵ_3	δ_3	δ_3	
ϵ_6	$\sigma_1 + \sigma_2$	δ_4	(3.21)

The different intersection of the fibers above yield the inequalities

$$\begin{aligned}
 \text{phase VI} \quad & \phi_3 < \phi_1 + \phi_6 \\
 & \phi_1 < \phi_6 \\
 \text{phase VII} \quad & \phi_6 < \phi_1.
 \end{aligned} \tag{3.22}$$

It can be easily checked that in both these phases the first two inequalities defining phase V in (3.19) hold. Also, the inequality defining phase VII implies $\phi_3 < \phi_1 + \phi_6$ showing that it is disjoint from VI.

So far we have constructed seven phases. The reflection symmetry of the E_6 Dynkin diagram means that for every phase found so far there exists another *distinct* phase in

which S_1 is exchanged with S_5 and S_2 is exchanged with S_4 . We will denote these as $\widetilde{\text{I}}, \widetilde{\text{II}}, \dots$. The defining inequalities of $\widetilde{\text{I}}, \widetilde{\text{II}}, \dots$ are obtained by making a $2 \leftrightarrow 4$ and $1 \leftrightarrow 5$ exchange in the those defining the $\text{I}, \text{II}, \dots$ phases. It is easily verified that the phases $\text{I}, \text{IV-VII}, \widetilde{\text{II}}$ and $\widetilde{\text{III}}$ completely cover the $\phi_5 < \phi_1$ region. It follows by symmetry that the complement of this region is covered by $\widetilde{\text{I}}, \text{II}, \text{III}$ and $\widetilde{\text{IV-VII}}$. We conclude therefore that all possible inequalities have been exhausted and the 14 disjoint phases found completely cover the Coulomb phase.

3.2. A prepotential calculation

The prepotential can be computed in each phase by evaluating all triple intersections of the form $S_i \cdot S_j \cdot S_k$. We carry this out in detail for the phase I defined in (3.5), all other cases being similar.

In order to obtain n_{27} quarks the divisors S_2 and S_4 must intersect S_3 along two sections, γ_1 and γ_2 , meeting transversely $n = n_{27}$ times. Since S_3 is minimally ruled, it must be isomorphic to \mathbf{F}_n and $\gamma_1 \simeq \gamma_2 \simeq C_3^\infty$. It follows that S_6 intersects S_3 along C_3^0 . This results in the intersection numbers

$$\begin{aligned} S_3 S_2^2 &= S_3 S_4^2 = n, & S_3 S_6^2 &= -n \\ S_3^2 S_2 &= S_3^2 S_4 = -n - 2, & S_3^2 S_6 &= n - 2, \end{aligned} \tag{3.23}$$

showing that

$$n_2 = n_4 = n + 2, \quad n_6 = n - 2. \tag{3.24}$$

Note that S_4 is obtained from \mathbf{F}_{n+2} by blowing-up $2n$ points lying at the intersection of n fibers with two distinct C_4^∞ sections. The strict transforms of the two sections are the holomorphic irreducible curves $C_4^\infty - \sum_{\alpha=1}^n \sigma_1^\alpha$ and $C_4^\infty - \sum_{\alpha=1}^n \sigma_3^\alpha$ [21]. The S_5 surface intersects S_4 along the former, therefore

$$S_4 S_5^2 = 2, \quad S_4^2 S_5 = -4. \quad n_5 = 4. \tag{3.25}$$

The other non-minimal surface is S_1 which is blown-up at $2n$ points lying at the intersection of n fibers with two sections C_1^0 and C_1^∞ . Therefore it intersects S_2 along the strict transform $C_1^0 - \sum_{\alpha=1}^n \sigma_1^\alpha$ in S_1 and along C_2^∞ in S_2 . It follows that

$$S_1^2 S_2 = n + 2, \quad S_1 S_2^2 = -n - 4, \quad n_1 = 4. \tag{3.26}$$

Recall that

$$S_2 \cdot S_4 = \sum_{\alpha=1}^n \delta^\alpha, \quad S_1 \cdot S_4 = \sum_{\alpha=1}^n \sigma_1^\alpha, \quad S_1 \cdot S_5 = \sum_{\alpha=1}^n \sigma_2^\alpha, \quad (3.27)$$

which determines

$$\begin{aligned} S_2^2 S_4 &= S_1 S_5^2 = -2n, \\ S_2 S_4^2 &= S_1^2 S_5 = 0, \\ S_1 S_4 S_5 &= S_1 S_2 S_4 = S_2 S_3 S_4 = n. \end{aligned} \quad (3.28)$$

Finally, the remaining intersection numbers are

$$S_2^3 = S_3^3 = S_5^3 = S_6^3 = 8, \quad S_1^3 = S_4^3 = 8 - 2n. \quad (3.29)$$

The prepotential, in this phase, determined by the intersection numbers (3.23)-(3.29) is given by

$$\begin{aligned} \mathcal{F} = & (8 - 2n)\phi_1^3 + 3(n + 2)\phi_1^2\phi_2 - 3(n + 4)\phi_1\phi_2^2 + 8\phi_2^3 + 3n\phi_2\phi_3^2 - 3(n + 2)\phi_2\phi_3^2 \\ & + 8\phi_3^3 - 3n\phi_1^2\phi_4 + 6n\phi_1\phi_2\phi_4 - 6n\phi_2^2\phi_4 + 6n\phi_2\phi_3\phi_4 - 3(n + 2)\phi_3^2\phi_4 - 3n\phi_1\phi_4^2 \\ & + 3n\phi_3\phi_4^2 + (8 - 2n)\phi_4^3 + 6n\phi_1\phi_4\phi_5 - 12\phi_4^2\phi_5 - 6n\phi_1\phi_5^2 + 6\phi_4\phi_5^2 + 8\phi_5^3 \\ & + 3(n - 2)\phi_3^2\phi_6 - 3n\phi_3\phi_6^2 + 8\phi_6^3 \end{aligned} \quad (3.30)$$

and agrees with the gauge theory result.

3.3. Fixed points analysis

The fixed point analysis is more involved than the previous cases and will be presented in detail. As shown in the first sub-section, the extended Kähler cone is divided into sub-cones, each corresponding to a smooth model. In each phase, we can contract the fibers and exceptional fiber components of the S_i obtaining a singular threefold \bar{X} with a curve of singularities \bar{C} as in [4]. Note that \bar{C} is the same for all phases. Since the contraction criterion establishes whether the curve \bar{C} can be further contracted in \bar{X} , it is enough to check it in a single phase which can be chosen arbitrarily. In the following we focus on the smooth model of phase I.

Consider a generic divisor

$$S = \sum_{i=1}^6 \phi_i S_i. \quad (3.31)$$

In phase I given by (3.5), the restrictions of S to the surfaces S_i are given by

$$\begin{aligned}
H_1 &\equiv -S \cdot S_1 = (2\phi_1 - \phi_2)C_1^\infty + (4\phi_2 - 2\phi_1 - n\phi_5)\epsilon_1 \\
&\quad - (\phi_1 + \phi_4 - \phi_2 - \phi_5) \sum_{\alpha=1}^n \sigma_1^\alpha - (\phi_1 - \phi_5) \sum_{\alpha=1}^n \sigma_3^\alpha \\
H_2 &\equiv -S \cdot S_2 = (2\phi_2 - \phi_1 - \phi_3)C_2^\infty + (2\phi_3 - n(\phi_2 + \phi_4 - \phi_3))\epsilon_2 \\
H_3 &\equiv -S \cdot S_3 = (2\phi_3 - \phi_2 - \phi_4 - \phi_6)C_3^\infty + (2\phi_3 - n(\phi_3 - \phi_6))\epsilon_3 \\
H_4 &\equiv -S \cdot S_4 = (2\phi_4 - \phi_3 - \phi_5)C_4^\infty + (2\phi_3 - n(\phi_2 + \phi_4 - \phi_3))\epsilon_4 \\
&\quad - (\phi_1 + \phi_4 - \phi_2 - \phi_5) \sum_{\alpha=1}^n \sigma_1^\alpha - (\phi_4 - \phi_2) \sum_{\alpha=1}^n \sigma_4^\alpha \\
H_5 &\equiv -S \cdot S_5 = (2\phi_5 - \phi_4)C_5^\infty + (4\phi_4 - 2\phi_5 - n\phi_1)\epsilon_5 \\
H_6 &\equiv -S \cdot S_6 = (2\phi_6 - \phi_3)C_6^\infty + (4 - n)\phi_6\epsilon_6.
\end{aligned} \tag{3.32}$$

As explained before, we have to check that for a generic divisor S the induced classes H_i are ample, and therefore must have positive intersection number with all irreducible holomorphic curves on S_i . We will actually check that H_i are positive with respect to all effective divisors on S_i . We start with the minimally ruled surfaces S_2 , S_3 , S_5 and S_6 . In these cases the H_i are ample if and only if the coefficients of C_i^∞ and ϵ_i are positive [21]. Taking into account the conditions (3.5), it follows that n must satisfy the bound $n \leq 3$. Note that all surfaces except S_6 actually allow $n \leq 4$.

Next we consider the blown-up surface S_1 . Since the Picard group of S_1 is generated by C_1^0 , ϵ_1 , σ_1^α and σ_3^α , an arbitrary divisor class can be written as

$$D_1 = a_1 C_1^0 + b_1 \epsilon_1 + \sum_{\alpha=1}^n c_\alpha \sigma_1^\alpha + \sum_{\alpha=1}^n d_\alpha \sigma_3^\alpha. \tag{3.33}$$

As showed in [22,23], if the class (3.33) has an effective representative, it must have non-negative intersection with all irreducible holomorphic curves C such that $C^2 \geq 0$. In particular, we can consider C to be one of the following

$$C_1^\infty, \quad \epsilon_1, \quad C_1^\infty - \sum_{\alpha=1}^n \sigma_3^\alpha, \quad C_1^\infty + n\epsilon_1 - \sum_{\alpha=1}^n \sigma_3^\alpha. \tag{3.34}$$

which yield the conditions

$$\begin{aligned} a_1 &\geq 0 \\ b_1 &\geq 0 \\ b_1 + \sum_{\alpha=1}^n d_\alpha &\geq 0 \\ b_1 + na_1 + \sum_{\alpha=1}^n c_\alpha &\geq 0. \end{aligned} \tag{3.35}$$

To check the ampleness of the class H_1 we rewrite D as

$$D = a_1 \left(C_1^0 - \sum_{\alpha=1}^n \sigma_1^\alpha \right) + b_1 (\sigma_1 + \sigma_2 + \sigma_3) + \sum_{\alpha=1}^n (a_1 + c_\alpha) \sigma_1^\alpha + \sum_{\alpha=1}^n d_\alpha \sigma_3^\alpha, \tag{3.36}$$

which gives

$$\begin{aligned} H_1 \cdot D_1 &= a_1 \left(C_1^0 - \sum_{\alpha=1}^n \sigma_1^\alpha \right) \cdot H_1 + \left(b_1 + na_1 + \sum_{\alpha=1}^n c_\alpha \right) H_1 \cdot \sigma_1 \\ &\quad + \left(b_1 + \sum_{\alpha=1}^n d_\alpha \right) H_1 \cdot \sigma_3 + b_1 H_1 \cdot \sigma_2. \end{aligned} \tag{3.37}$$

It can be checked by direct computation that inside the sub-cone (3.5), all the intersections appearing in (3.37) are positive for $n \leq 4$. Therefore, using the conditions (3.35), we find that H_1 restricts to an ample class on S_1 when $n \leq 4$.

Finally, we consider the class H_4 . A generic divisor on S_4 is given by

$$D_4 = a_4 C_4^0 + b_4 \epsilon_4 + \sum_{\alpha=1}^n c_\alpha \sigma_1^\alpha + \sum_{\alpha=1}^n d_\alpha \sigma_4^\alpha. \tag{3.38}$$

The conditions on the coefficients imposed by requiring the class (3.38) to have an effective representative are

$$\begin{aligned} a_4 &\geq 0 \\ b_4 &\geq 0 \\ b_1 + \sum_{\alpha=1}^n c_\alpha &\geq 0 \\ b_1 + \sum_{\alpha=1}^n d_\alpha &\geq 0. \end{aligned} \tag{3.39}$$

These are derived using the holomorphic, positive self-intersection curves

$$C_4^\infty, \quad \epsilon_4, \quad C_4^\infty - \sum_{\alpha=1}^n \sigma_1^\alpha, \quad C_4^\infty - \sum_{\alpha=1}^n \sigma_4^\alpha. \quad (3.40)$$

After a similar manipulation as above, we get

$$H_4 \cdot D_4 = a_4 C_0 \cdot H_4 + \left(b_4 + \sum_{\alpha=1}^n c_\alpha \right) \sigma_1 \cdot H_4 + \left(b_4 + \sum_{\alpha=1}^n d_\alpha \right) \sigma_4 \cdot H_4 + b_4 \delta \cdot H_4. \quad (3.41)$$

As before, it can be easily shown that for classes H_4 inside the sub-cone (3.5) all the intersections in (3.41) are positive if $n \leq 4$. Together with the condition (3.39) this implies that H_4 restricts to an ample class on S_4 if $n \leq 4$.

The end result is that the classes $H_i = -S \cdot S_i$ are ample for any divisor S inside the sub-cone if $n \leq 3$. We conclude that for these values of $n = n_{27}$ there exist UV fixed points with E_6 gauge symmetry.

4. E_7 with n_{56} quarks

4.1. Degenerations and phase structure

An E_7 degeneration can be similarly constructed by performing canonical resolution of the corresponding F-theory Weierstrass model (appendix C). The result is represented below.

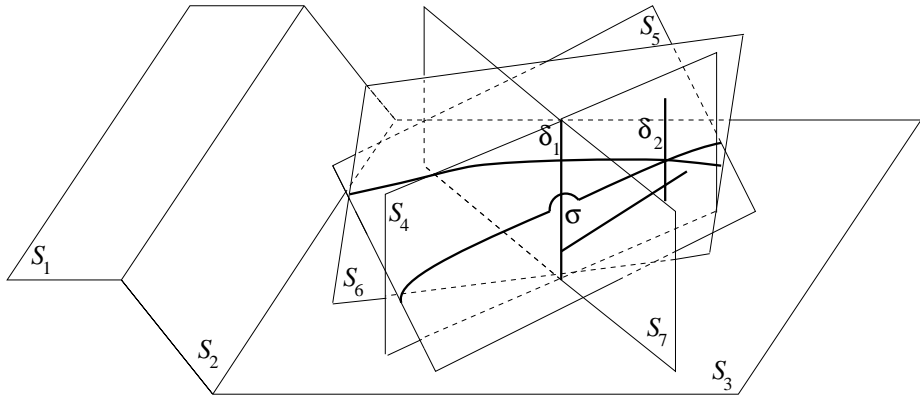


Fig. 8: E_7 degeneration - phase I

All surfaces except S_4 are minimally ruled over rational curves. The base of S_4 is also rational but the surface is obtained from a minimal ruling by blowing-up two distinct points on a given fiber. The result is a reducible fiber with three components

$$\epsilon_4 = \delta_1 + 2\sigma + \delta_2. \quad (4.1)$$

Note that S_4 and S_7 intersect along the curve δ_1 which is a fiber in the ruling of S_7 . Similarly, S_4 and S_6 intersect along the curve δ_2 which is a fiber in the ruling of S_6 . This is consistent with the embedding in the ambient Calabi-Yau space only if δ_1, δ_2 are (-2) curves and σ is a (-1) curve on S_4 . A local computation (appendix A) shows that this is indeed the case. The intersection matrix of δ_1, δ_2 and σ with the exceptional divisors is

	S_3	S_4	S_5	S_6	S_7
δ_1	1	0	0	0	-2
δ_2	0	0	1	-2	0
σ	0	-1	0	1	1

(4.2)

From (4.1) and (4.2) it follows that $\epsilon_i \cdot S_j$ reproduces the E_7 Cartan matrix. At the same time, σ is a weight vector of the **56** representation and all other vectors can be obtained by taking linear combinations with the fiber classes ϵ_i .

The **56** representation of E_7 is pseudo-real, inducing a split of its weight vectors into two sets Δ_{\pm} , such that if $v \in \Delta_+$, $(-v) \in \Delta_-$. Hypermultiplets coming from anti-membranes wrapping curves associated to weight vectors in Δ_- are therefore related to those arising from membranes wrapping curves in Δ_+ , so a single holomorphic curve gives rise to a half-hypermultiplet. Since $\pi_4(E_7)$ is trivial, the E_7 gauge theory is not afflicted with a global anomaly, permitting an odd number of half-hypermultiplets. This should be reflected in the geometry, and indeed the weight σ need not appear in pairs. It is also consistent with the Weierstrass model considered in appendix C.

Theories with n half-hypermultiplets can be engineered by colliding the surfaces S_4 and S_7 n times along distinct fibers $\delta_1^1, \dots, \delta_1^n$ in the ruling of S_7 . This introduces n reducible fibers

$$\epsilon^\alpha = \delta_1^\alpha + 2\sigma^\alpha + \delta_2^\alpha, \quad \alpha = 1, \dots, n \quad (4.3)$$

in the ruling of S_4 .

As in the E_6 case, the degeneration described in fig. 8 is not unique and the relative Kähler cone admits a subdivision into sub-cones corresponding to different geometric

phases. To see that note that the present sub-cone, labeled phase I, is defined as the intersection of the extended cone

$$-S \cdot \epsilon_i > 0 \quad (4.4)$$

with the hyper-cone

$$-S \cdot \sigma > 0 \quad (4.5)$$

which gives

$$\phi_6 + \phi_7 < \phi_4. \quad (4.6)$$

We now proceed to uncover the phase structure as in the E_6 case. Since the E_7 Dynkin diagram does not have the symmetry of the E_6 one, we will have to enumerate all the phases explicitly.

Phase II - The degeneration of this phase is described in fig. 9 below.

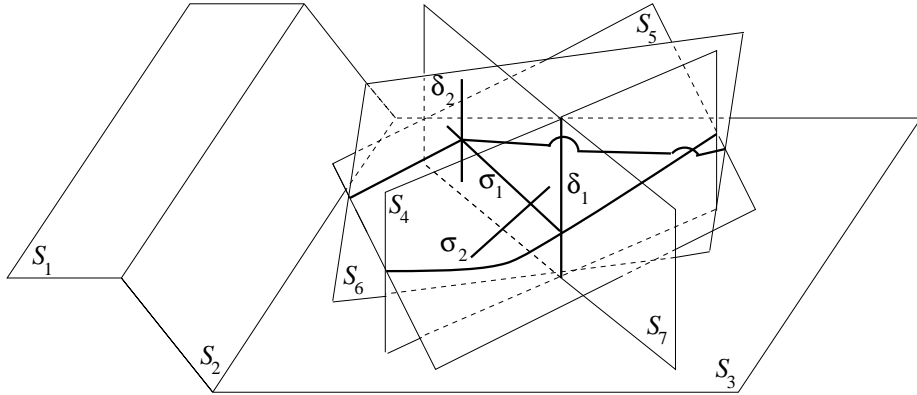


Fig. 9: E_7 degeneration - phase II

All surfaces are minimally ruled except for S_5 and S_7 . S_7 has a reducible fiber with three components

$$\epsilon_7 = \delta_1 + 2\sigma_1 + \delta_2 \quad (4.7)$$

where δ_1, δ_2 are (-2) curves and σ_1 is a (-1) curve. S_5 has a reducible fiber with two components

$$\epsilon_5 = \sigma_1 + \sigma_2 \quad (4.8)$$

where both σ_1 and σ_2 are (-1) curves. Note that S_4 and S_7 intersect along δ_1 which is a fiber in the ruling of S_4 . S_5 and S_7 intersect along σ_1 and S_6 and S_7 intersect along δ_2

which is a fiber in the ruling of S_6 . The intersection matrix of $\delta_1, \delta_2, \sigma_1$ and σ_2 with the exceptional divisors is

	S_3	S_4	S_5	S_6	S_7	
δ_1	1	-2	1	0	0	
δ_2	0	0	1	-2	0	
σ_1	0	1	-1	1	-1	
σ_2	0	0	-1	0	1	(4.9)

It is easily verified that (4.8) and (4.9) yield the correct Cartan matrix and that σ_1, σ_2 are weight vectors of **56**. The inequalities which define this sub-cone can be read off from (4.9) and (4.5),

$$\begin{aligned} \phi_4 + \phi_6 &< \phi_5 + \phi_7, \\ \phi_7 &< \phi_5. \end{aligned} \tag{4.10}$$

By adding ϕ_6 to first line above and using the inequality $2\phi_6 - \phi_5 > 0$ which holds everywhere in the external cone we get $\phi_4 < \phi_6 + \phi_7$. This shows that phases I and II are indeed disjoint.

Phase III - The present phase can be immediately obtained from the previous one by flopping σ_5 from S_5 to S_7 . This gives the cone

$$\begin{aligned} \phi_4 + \phi_6 &< \phi_5 + \phi_7, \\ \phi_5 &< \phi_7. \end{aligned} \tag{4.11}$$

The first inequality above is actually redundant. This can be seen by adding ϕ_5 to both sides of the second inequality and using $2\phi_5 - \phi_4 - \phi_6 > 0$ which defines the external cone to get the first inequality in (4.11). We can therefore show, as in phase II, that phases I and III are disjoint.

So far, we have constructed three disjoint phases. The complement of these three sub-cones in the extended Kähler cone is defined by

$$\begin{aligned} \phi_4 &< \phi_6 + \phi_7, \\ \phi_5 + \phi_7 &< \phi_4 + \phi_6, \end{aligned} \tag{4.12}$$

and we will have to verify that the inequalities defining the phases below cover this region completely.

Phase IV - The degeneration corresponding to this phase is described in the figure below.

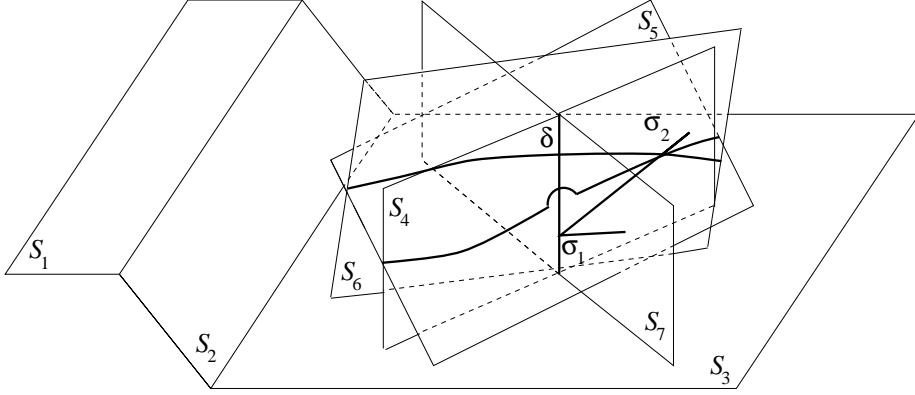


Fig. 10: E_7 degeneration - phase IV

In this sub-cone, S_4 , S_6 and S_7 are minimally ruled surfaces blown-up in n distinct points. The n reducible fibers are

$$\begin{aligned}\epsilon_4^\alpha &= \delta^\alpha + \sigma_2^\alpha \\ \epsilon_6^\alpha &= \sigma_1^\alpha + \sigma_2^\alpha \\ \epsilon_7^\alpha &= \delta^\alpha + \sigma_1^\alpha.\end{aligned}\tag{4.13}$$

Note that

$$S_4 \cap S_7 \simeq \sum_{\alpha=1}^n \delta^\alpha, \quad S_4 \cap S_6 \simeq \sum_{\alpha=1}^n \sigma_2^\alpha, \quad S_6 \cap S_7 \simeq \sum_{\alpha=1}^n \sigma_1^\alpha.\tag{4.14}$$

The intersection matrix of δ , σ_1 and σ_2 is

	S_3	S_4	S_5	S_6	S_7
δ	1	-1	0	1	-1
σ_1	0	1	0	-1	-1
σ_2	0	-1	1	-1	1

(4.15)

Thus the inequalities defining this phase are

$$\begin{aligned}\phi_3 + \phi_6 &< \phi_4 + \phi_7, \\ \phi_4 &< \phi_6 + \phi_7, \\ \phi_5 + \phi_7 &< \varphi_4 + \phi_6.\end{aligned}\tag{4.16}$$

Phase V - The degeneration is described fig. 11 below.

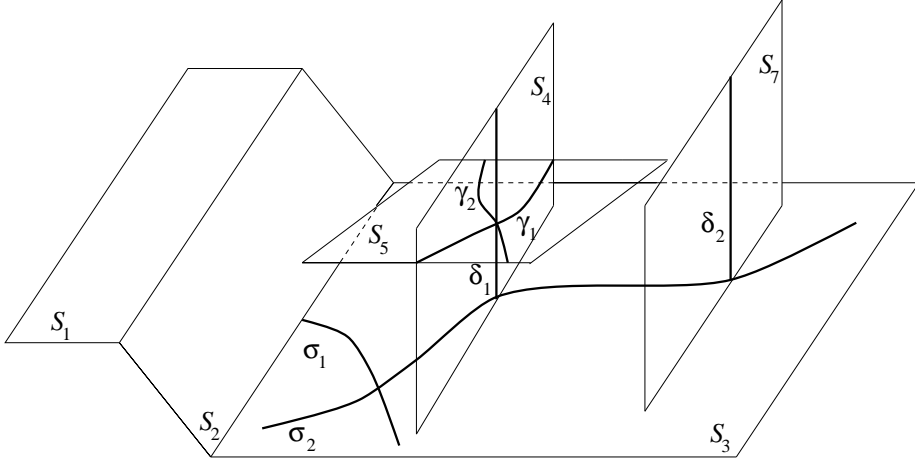


Fig. 11: E_7 degeneration - phase V

All surfaces are minimally ruled except for S_3 and S_6 which is too complicated to draw, but intersects S_5 along γ_2 . The reducible fibers are given by

$$\begin{aligned}\epsilon_3 &= \sigma_1 + \sigma_2 \\ \epsilon_6 &= \delta_1 + \delta_2 + 2\sigma_2.\end{aligned}\tag{4.17}$$

σ_1 is a (-1) curve in S_3 and σ_2 is a (-1) curves in both S_3 and S_6 . δ_1 and δ_2 are (-2) curves in S_6 . The intersection matrix is given by

$$\begin{array}{c|ccccccc|c}\hline & S_2 & S_3 & S_4 & S_5 & S_6 & S_7 \\ \hline \delta_1 & 0 & 1 & -2 & 1 & 0 & 0 \\ \delta_2 & 0 & 1 & 0 & 0 & 0 & -2 \\ \sigma_1 & 1 & -1 & 0 & 0 & 1 & 0 \\ \sigma_2 & 0 & -1 & 1 & 0 & -1 & 1 \\\hline\end{array},\tag{4.18}$$

from which we can read the inequalities

$$\begin{aligned}\phi_4 + \phi_7 &< \phi_3 + \phi_6 \\ \phi_2 + \phi_6 &< \phi_3.\end{aligned}\tag{4.19}$$

It is easy to verify that this sub-cone is inside the complement of phases I, II and III. Adding ϕ_7 to both sides of the first inequality in (4.19) and using the ϵ_7 inequality in (4.4) leads to the first inequality in (4.12). Doing the same with $7 \rightarrow 4$ leads to the second inequality in (4.12).

Phases VI, VII and VIII - These phases are obtained by flopping σ_2 first to S_2 then to S_1 and finally outside S_1 .

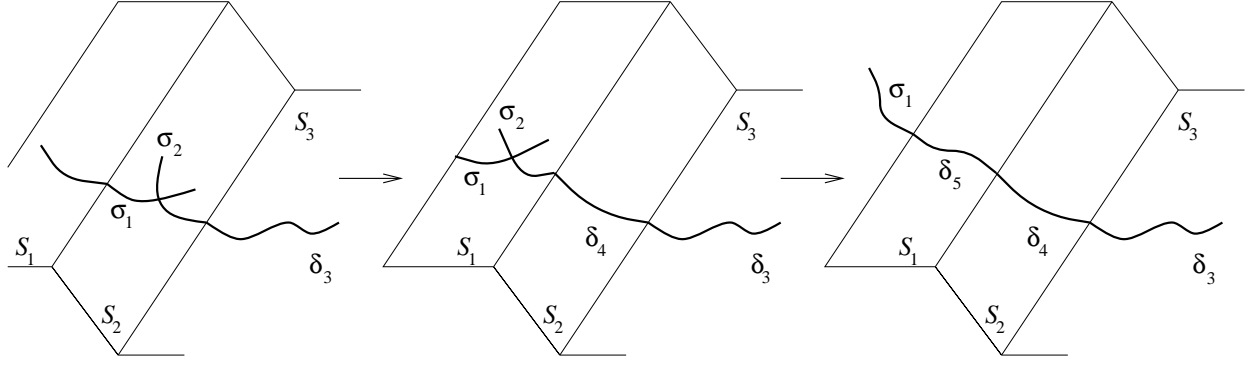


Fig. 12: E_7 degenerations - phases VI, VII and VIII

The geometry of these degenerations is identical to that of phase V with the following differences:

	phase VI	phase VII	phase VIII
ϵ_1	ϵ_1	$\sigma_1 + \sigma_2$	δ_5
ϵ_2	$\sigma_1 + \sigma_2$	δ_4	δ_4
ϵ_3	δ_3	δ_3	δ_3
ϵ_6	$\delta_1 + \delta_2 + 2\delta_3$ + $2\sigma_2$	$\delta_1 + \delta_2 + 2\delta_3$ + $2\delta_4 + 2\sigma_2$	$\delta_1 + \delta_2 + 2\delta_3$ + $2\delta_4 + 2\delta_5$

(4.20)

It is straight forward to check how the intersection numbers of the curves $\sigma_{1,2}$ change as the double fiber is flopped from phase V to phase VIII. We find the following inequalities

$$\begin{array}{ll}
 \text{phase VI} & \phi_3 < \phi_2 + \phi_6 \\
 & \phi_1 + \phi_6 < \phi_2 \\
 \text{phase VII} & \phi_2 < \phi_1 + \phi_6 \\
 & \phi_6 < \phi_1 \\
 \text{phase VIII} & \phi_1 < \phi_6.
 \end{array} \tag{4.21}$$

The calculation showing that all these phases are mutually disjoint as well as disjoint from the previous ones is easy and will not be repeated here.

To summarize, in the presence of massless **56** matter multiplets, the E_7 Coulomb branch is divided into eight phases determined by the inequalities (4.6), (4.10), (4.11), (4.16), (4.19) and (4.21).

4.2. A prepotential calculation

We calculate the prepotential in phase IV defined in (4.16). The triple intersections of this configuration can be computed as follows. S_4 and S_7 intersect S_3 along two sections meeting transversely n times. As S_3 is minimally ruled, it follows that it must be isomorphic to \mathbf{F}_n and the two sections are in the C_3^∞ class. S_2 does not intersect S_4 and S_7 , therefore it must meet S_3 along C_3^0 . This results in the intersection numbers

$$\begin{aligned} S_3S_4^2 &= S_3S_7^2 = n, & S_3S_2^2 &= -n \\ S_3^2S_4 &= S_3^2S_7 = -n - 2, & S_3^2S_2 &= n - 2. \end{aligned} \tag{4.22}$$

It is then easy to compute

$$S_1^2S_2 = 2 - n, \quad S_1S_2^2 = n - 4. \tag{4.23}$$

Since S_1 and S_2 intersect along C_1^∞ on S_1 and C_2^0 on S_2 , the degrees of the rulings are

$$n_1 = n - 4, \quad n_2 = n - 2, \quad n_4 = n_7 = n + 2. \tag{4.24}$$

Note that the non-minimal surfaces S_4 , S_6 and S_7 are obtained from minimal rulings by blowing-up the intersection points of n fibers with a section in C^∞ . Therefore, S_4 and S_5 intersect along the strict transform $C_4^\infty - \sum_{\alpha=1}^n \sigma_2^\alpha$ on S_4 and C_5^0 on S_5 . It follows that

$$S_4S_5^2 = 2, \quad S_4^2S_5 = -4, \quad n_5 = 4. \tag{4.25}$$

The intersections (4.14) determine

$$\begin{aligned} S_4^2S_7 &= S_4S_7^2 = -n & S_3S_4S_7 &= n \\ S_4^2S_6 &= S_4S_6^2 = -n & S_4S_6S_7 &= n \\ S_6^2S_7 &= S_6S_7^2 = -n & S_4S_5S_6 &= n. \end{aligned} \tag{4.26}$$

S_4 and S_6 intersect S_5 along two sections meeting in n points lying on the curves σ_2^α . Since $n_5 = 4$, the two sections must be C_5^0 and $C_5^\infty + n\epsilon_5$ respectively. This implies that

$$S_5S_6^2 = 2n + 4, \quad S_5^2S_6 = -2n - 6, \quad n_6 = 2n + 6. \tag{4.27}$$

Finally, the remaining intersection numbers are

$$S_1^3 = S_2^3 = S_3^3 = S_5^2 = 8, \quad S_4^3 = S_6^3 = S_7^3 = 8 - n. \tag{4.28}$$

The intersection numbers (4.22)-(4.28) lead to the prepotential

$$\begin{aligned} \mathcal{F} = & 8\phi_1^3 - 3(n-2)\phi_1^2\phi_2 + 3(n-4)\phi_1\phi_2^2 + 8\phi_2^3 - 3n\phi_2^2\phi_3 + 3(n-2)\phi_2\phi_3^2 + 8\phi_3^3 \\ & - 3(n+2)\phi_3^2\phi_4 + 3n\phi_3\phi_4^2 + (8-n)\phi_4^3 - 12\phi_4^2\phi_5 + 6\phi_4\phi_5^2 + 8\phi_5^3 - 3n\phi_4^2\phi_6 + 6n\phi_4\phi_5\phi_6 \\ & - 3(2n+6)\phi_5^2\phi_6 - 3n\phi_4\phi_6^2 + 3(2n+4)\phi_5\phi_6^2 + (8-n)\phi_6^3 - 3(n+2)\phi_3^2\phi_7 + 6n\phi_3\phi_4\phi_7 \\ & - 3n\phi_4^2\phi_7 + 6n\phi_4\phi_6\phi_7 - 3n\phi_6^2\phi_7 + 3n\phi_3\phi_7^2 - 3n\phi_4\phi_7^2 - 3n\phi_6\phi_7^2 + (8-n)\phi_7^3 \end{aligned} \tag{4.29}$$

This agrees with the gauge theory computation for this phase.

4.3. Fixed points analysis

The fixed point analysis follows the same lines as in the E_6 case and we shall do it in phase IV. Let

$$S = \sum_{i=1}^7 \phi_i S_i \quad (4.30)$$

denote a generic divisor in the sub-cone (4.16). The restrictions of S to the surfaces S_i are

$$\begin{aligned} H_1 &\equiv -S \cdot S_1 = (2\phi_1 - \phi_2)C_1^\infty + \phi_1(6 - n)\epsilon_1 \\ H_2 &\equiv -S \cdot S_2 = (2\phi_2 - \phi_1 - \phi_3)C_2^\infty + (4\phi_2 - 2\phi_1 - n(\phi_2 - \phi_1))\epsilon_2 \\ H_3 &\equiv -S \cdot S_3 = (2\phi_3 - \phi_2 - \phi_4 - \phi_7)C_3^\infty + (2\phi_3 - n(\phi_3 - \phi_2))\epsilon_3 \\ H_4 &\equiv -S \cdot S_4 = (2\phi_4 - \phi_3 - \phi_5)C_4^\infty + (2\phi_3 - n(\phi_4 + \phi_7 - \phi_3))\epsilon_4 \\ &\quad - (\phi_4 + \phi_6 - \phi_5 - \phi_7) \sum_{\alpha=1}^n \sigma_2^\alpha \\ H_5 &\equiv -S \cdot S_5 = (2\phi_5 - \phi_4 - \phi_6)C_5^\infty + (4\phi_4 - 2\phi_5 - n\phi_6)\epsilon_5 \\ H_6 &\equiv -S \cdot S_6 = (2\phi_6 - \phi_5)C_6^\infty + (6\phi_5 - 4\phi_6 - n(2\phi_6 - 2\phi_5 + \phi_4))\epsilon_6 \\ &\quad - (\phi_6 + \phi_7 - \phi_4) \sum_{\alpha=1}^n \sigma_1^\alpha \\ H_7 &\equiv -S \cdot S_7 = (2\phi_7 - \phi_3)C_7^\infty + (2\phi_3 - n(\phi_7 - \phi_3 + \phi_4))\epsilon_7 \\ &\quad - (\phi_6 + \phi_7 - \phi_4) \sum_{\alpha=1}^n \sigma_1^\alpha. \end{aligned} \quad (4.31)$$

We first check ampleness on the minimally ruled surfaces S_1, S_2, S_3 and S_5 . Taking into account the inequalities (4.16) defining the phase, this yields the bound $n \leq 5$. Note that all surfaces allow $n = 6$ except for S_1 .

Next, we consider the blown-up surface S_4 . As in the previous section, a generic divisor class can be written

$$D_4 = a_4 C_4^0 + b_4 \epsilon_4 + \sum_{\alpha=1}^n c_\alpha \sigma_2^\alpha. \quad (4.32)$$

If this class admits an effective representative, it must have non-negative intersection number with all irreducible holomorphic curves C such that $C^2 \geq 0$. Checking that this condition holds for the curves

$$C_4^\infty, \quad \epsilon_4, \quad C_4^\infty - \sum_{\alpha=1}^n \sigma_2^\alpha \quad (4.33)$$

gives the restrictions

$$\begin{aligned} a_4 &\geq 0 \\ b_4 &\geq 0 \\ b_4 + \sum_{\alpha=1}^n c_\alpha &\geq 0. \end{aligned} \tag{4.34}$$

The intersection numbers of H_4 with C_4^0, σ_4 and δ are easily seen to be positive inside the sub-cone (4.16) when $n \leq 6$. Using the conditions (4.34) we then find that H_4 is restricts to an ample class on S_4 if $n \leq 6$. The analysis of H_6 and H_7 is identical and gives the same restriction on n .

In conclusion, we find that H_i is ample on each surface S_i if $n \leq 5$. Therefore for $n_{56} = \frac{n}{2} \leq \frac{5}{2}$ there exist UV fixed points with E_7 gauge symmetry.

Acknowledgments

We would like to thank Kenneth Intriligator, Ori Ganor, Barak Kol, Luboš Motl, David Morrison, Christian Römer, Nathan Seiberg and especially Cumrun Vafa for helpful discussions. We are very grateful to Cumrun Vafa for suggesting the idea of this work.

Appendix A. Ruled Surfaces, Blow-ups and All That

This is a brief exposition of basic properties of ruled surfaces and their monoidal transformations used throughout the paper. These facts can be found in any mathematical monograph on the subject. Our presentation follows [21].

A ruled surface is a smooth complex projective surface S with a fibration structure $\pi : S \rightarrow C$ where C is a smooth curve of genus g and the fibers of π are isomorphic to \mathbf{P}^1 . In general, S can be represented as the projectivization of a rank two holomorphic vector bundle E on C . The degree $n = -\deg E$ is an invariant of S .

The Picard group of S contains two distinguished section classes, C_0 and C_∞ , and a fiber class f . They satisfy

$$\begin{aligned} C_0^2 &= -n, & f^2 &= 0, & C_0 \cdot f &= 1 \\ C_\infty &= C_0 + nf & \Rightarrow & C_\infty \cdot C_0 &= 0, & C_\infty \cdot f &= 1. \end{aligned} \tag{A.1}$$

Note that the two sections are disjoint and

$$C_0^2 + C_\infty^2 = 0. \tag{A.2}$$

The canonical class of S is given by

$$K_S = -2C_0 - (n+2)f = -2C_\infty + (n-2)f. \quad (\text{A.3})$$

Other surfaces occurring in many examples in the main text are simply obtained by blowing-up the points $P_1, \dots, P_k \in S$ lying at the intersection of k fibers with a given section γ . The latter can be either C_0 or C_∞ . For concreteness, we consider $\gamma \simeq C_\infty$. The resulting surface, \tilde{S}_1 , can be regarded as fibration over C with a reducible fiber with two components

$$f = e_1 + e'_1 = \dots = e_k + e'_k \quad (\text{A.4})$$

over P_1, \dots, P_k as in fig. 13.

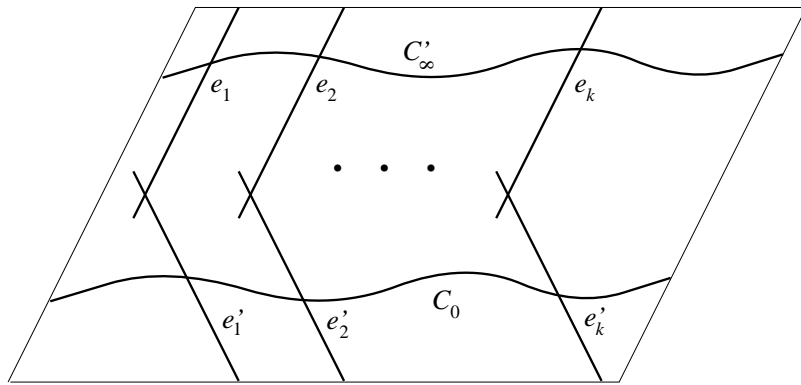


Fig. 13: Blowing-up k points lying on C_∞ .

The fiber components satisfy the intersection relations

$$\begin{aligned} e_i \cdot e_j &= e'_i \cdot e'_j = -\delta_{ij}, & e_i \cdot e'_j &= \delta_{ij} \\ e_i \cdot C_0 &= e_i \cdot C_\infty = 0, & e'_i \cdot C_0 &= 1. \end{aligned} \quad (\text{A.5})$$

The strict transform of C_∞ is

$$C'_\infty = C_\infty - \sum_{i=1}^k e_i, \quad (\text{A.6})$$

satisfying

$$e_i \cdot C'_\infty = 1, \quad e'_i \cdot C'_\infty = 0. \quad (\text{A.7})$$

Note also that

$$C_0^2 + C'_\infty^2 = -k. \quad (\text{A.8})$$

The canonical class of \tilde{S}_1 is given by

$$K_{\tilde{S}_1} = -2C_0 - (n+2)f + \sum_{i=1}^k e_i. \quad (\text{A.9})$$

This example can be generalized in a number of ways, which are important for the degenerations in section three and four. We can blow-up a pair of points of intersection of each of the above k fibers with two distinct sections. The latter can be again chosen to be C_0, C_∞ or two sections in C_∞ (corresponding respectively to surfaces S_1 and S_4 in section 3.2).

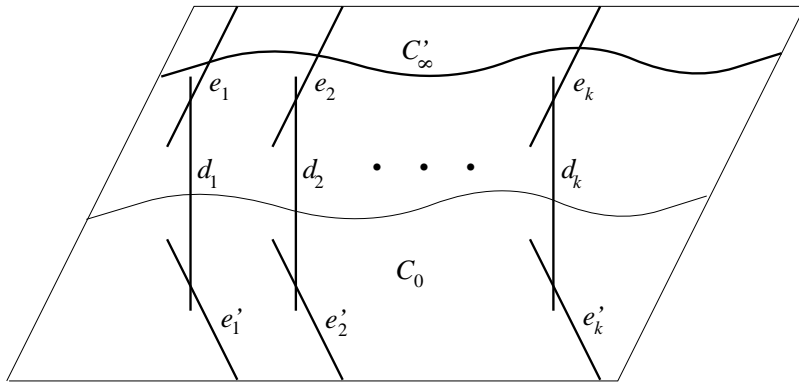


Fig. 14: Blowing-up $2k$ points lying on two C_∞ sections.

This results in k reducible fibers with three components

$$f = e_1 + d_1 + e'_1 = \dots = e_k + d_k + e'_k. \quad (\text{A.10})$$

The new intersection numbers are

$$\begin{aligned} e_i \cdot e_j &= e'_i \cdot e'_j = -\delta_{ij}, \\ d_i \cdot d_j &= -2\delta_{ij}, \quad e_i \cdot d_j = e'_i \cdot d_j = \delta_{ij}. \end{aligned} \quad (\text{A.11})$$

Note that the strict transforms of the original fibers d_i must now be (-2) curves. The original sections C_0 and C_∞ do not meet the exceptional components e_i or e'_i . The canonical class of this surface is now given by

$$K_{\tilde{S}_2} = -2C_0 - (n+2)f + \sum_{i=1}^k (e_i + e'_i). \quad (\text{A.12})$$

This construction is relevant for phase I of the E_6 degeneration. Phases III and V-VII involve reducible fibers of the form $f = e + d_1 + \dots + d_k + e'$ where e, e' are (-1) curves and d_i are (-2) curves. These can be realized by successive blow-ups.

Alternatively, we can blow-up the k points of intersection of the fiber components in fig. 13. The resulting surface has k reducible fibers with three components

$$f = e_1 + 2d_1 + e'_1 = \dots = e_k + 2d_k + e'_k. \quad (\text{A.13})$$

Here e_i and e'_i are proper transforms of the original fiber components while d_i are (-1) curves induced by the blow-up. Their intersection matrix is given by

$$\begin{aligned} e_i \cdot e_j &= e'_i \cdot e'_j = -2\delta_{ij}, \\ d_i \cdot d_j &= -\delta_{ij}, \quad e_i \cdot d_j = e'_i \cdot d_j = \delta_{ij}. \end{aligned} \quad (\text{A.14})$$

Note that d_i appear with multiplicity 2 in the fiber so that $f^2 = 0$ is satisfied. The original sections C_0 and C_∞ intersect e'_i but not the other fiber components. Different sections passing through the fiber components can be defined as in (A.6). The canonical class of the new surface \tilde{S}_3 is given by

$$K_{\tilde{S}_3} = -2C_0 - (n+2)f + \sum_{i=1}^k (2d_i + e_i). \quad (\text{A.15})$$

Phases VI-VIII in section four require reducible fibers of the form $f = d_1 + d_2 + 2d_3 + \dots + 2d_k + 2e$ where d_i are (-2) curves and e is a (-1) curve. This can be realized by successive blow-ups of \tilde{S}_3 .

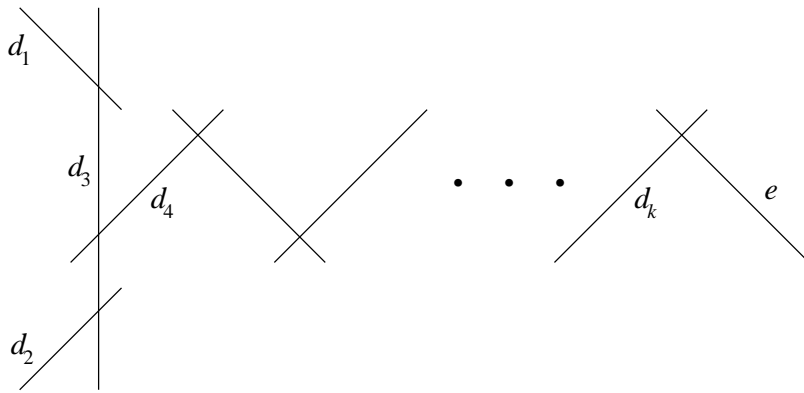


Fig. 15: Reducible fiber for the E_7 phases V-VIII.

We end this section with some comments on triple intersections in Calabi-Yau degenerations. The neighborhood of any surface S embedded in a smooth Calabi-Yau threefold X is isomorphic to the total space of the canonical bundle of S . Therefore the intersection numbers are determined by local data

$$S^3 = K_S^2. \quad (\text{A.16})$$

This gives $S^3 = 8$ for a minimally ruled surface. Equations (A.9), (A.12) and (A.15) show that S^3 decreases by 1 for each blow-up of S

$$\tilde{S}_1^3 = 8 - k, \quad \tilde{S}_2^3 = \tilde{S}_3^3 = 8 - 2k. \quad (\text{A.17})$$

Next, if two surfaces S_1, S_2 intersect transversely along a curve γ we have

$$S_1^2 S_2 = (\gamma^2)_{S_2}, \quad S_1 S_2^2 = (\gamma^2)_{S_1}. \quad (\text{A.18})$$

The embedding in the Calabi-Yau space requires

$$S_1^2 S_2 + S_1 S_2^2 = \deg(N_{\gamma/S}) = 2g - 2 \quad (\text{A.19})$$

where g is the genus of γ . Combined with (A.8), these are the basic elements entering the prepotential computations in the main text.

Appendix B. Resolution of the E_6 Weierstrass Model

We consider six dimensional F theory compactified on a singular Weierstrass model over \mathbf{F}_n base described by the equation

$$y^2 = x^3 + x f(z_1, z_2) + g(z_1, z_2). \quad (\text{B.1})$$

Here z_1, z_2 are affine coordinates on the \mathbf{P}^1 fiber and \mathbf{P}^1 base of the Hirzebruch surface. According to [16], the Weierstrass model exhibits a split E_6 singularity along the section $z_1 = 0$ of \mathbf{F}_n if

$$\begin{aligned} f(z_1, z_2) &= z_1^3 f_{8+n}(z_2) \\ g(z_1, z_2) &= z_1^4 q_{n+6}^2(z_2) + z_1^5 g_{12+n}(z_2) \end{aligned} \quad (\text{B.2})$$

where the subscripts indicate the degrees of the polynomials. The discriminant of the elliptic fibration is

$$\Delta = z_1^8 (27 q_{n+6}(z_2)^4 + O(z_1)). \quad (\text{B.3})$$

Therefore the line $z_1 = 0$ of IV^* singularities intersects a line of I_1 singularities at the zeroes of q_{n+6} . Based on the dual heterotic model, each zero of q_{n+6} is expected to yield a hypermultiplet in the **27** representation. We will explicitly check this prediction by constructing a smooth model of the singular elliptic fibration as in [17,19].

Introducing local coordinates (t, s) near a simple zero of q_{n+6} , the singularity can be written

$$y^2 = x^3 + s^3x + s^4t^2. \quad (\text{B.4})$$

In these coordinates, we have

$$f = s^3, \quad g = s^4t^2, \quad \Delta = s^8(4s + 27t^4). \quad (\text{B.5})$$

The vanishing degrees along the line $s = 0$ in the base are $(3, 4, 8)$ therefore this is a line of IV^* fibers. The vanishing degrees along $4s + 27t^4 = 0$ are $(0, 0, 1)$ therefore this is a line of I_1 fibers colliding $s = 0$ at $s = t = 0$. At the collision locus, the degrees jump to $(3, 6, 9)$ which characterize a III^* fiber. Although the collision is not transverse, we can still apply the resolution scheme of [17] (see the appendix of [19]). The elliptic fibration can be represented as a double cover of a $\mathbf{P}^1(x)$ fibration over the (s, t) plane branched over the surface B

$$x^3 + s^3x + s^4t^2 = 0. \quad (\text{B.6})$$

The problem can be reduced to the elliptic surface case by considering certain slices through various points of the discriminant [19]. For fixed $t \neq 0$ this is a singularity of analytic type $x^3 + s^4$ describing the generic IV^* fiber. For $t = 0$, the singularity is of analytic type $x^3 + s^3x$ corresponding to a III^* fiber. The resolution proceeds by successively blowing up the $x = s = 0$ line until the generic IV^* singularity is resolved. The III^* fiber over $s = t = 0$ is only partially resolved after this process. The intermediate steps are represented in fig. 16 and fig. 17. According to the conventions of [17,19], dotted line segments represent unbranched rational curves and solid line segments represent branched exceptional rational curves. The curved lines represent the proper transform of the original branch locus. The leftmost dotted vertical line always represents the proper transform of the original fiber of the ruling. In the M theory limit, this component grows to infinite size. The curves $f_1 \dots f_4$ are fibers of the exceptional ruled surfaces $\mathbf{F}_1, \dots, \mathbf{F}_4$ over the t -line. Note that the proper transform \tilde{B} of the branch surface intersects \mathbf{F}_1 and \mathbf{F}_2 transversely along the fibers \mathbf{F}_1 and \mathbf{F}_2 over $s = t = 0$. The surface \mathbf{F}_4 is branched while \mathbf{F}_3 intersects the branch locus along two sections.

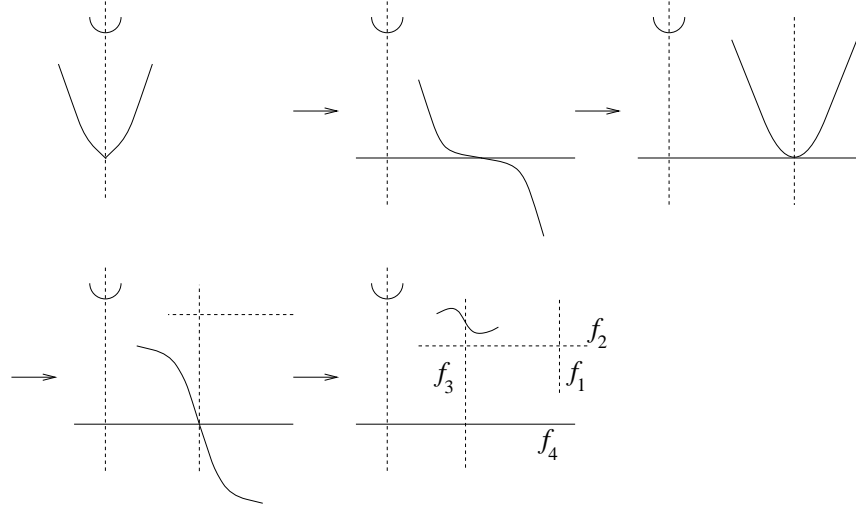


Fig. 16: Resolution of the generic IV^* fiber.

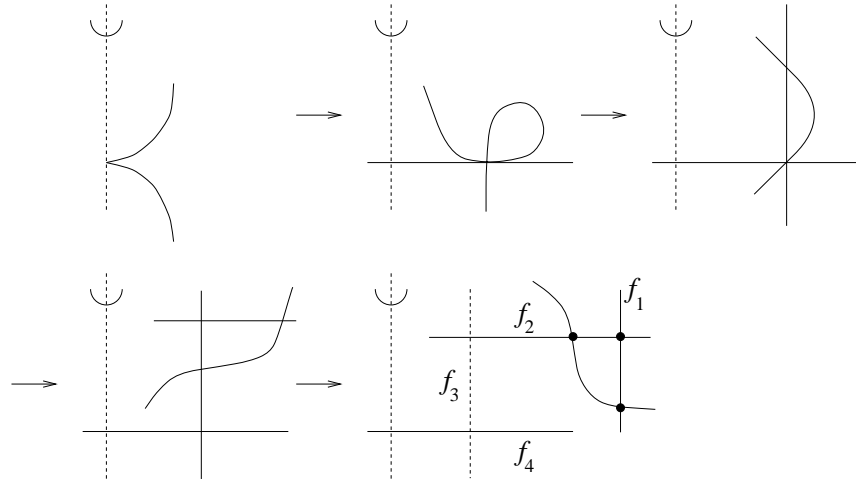


Fig. 17: Partial resolution of the III^* fiber over the collision locus.

The three marked points in the last diagram in fig. 17. represent three double point singularities of \tilde{B} of analytic type $uv = w^2$ in certain coordinates (u, v, w) on the blow-up. Therefore the threefold is still singular at this point. In order to construct a smooth model, one has to blow-up the three singular points [17] introducing three exceptional \mathbf{P}^2 divisors as in fig. 18.a.

The surface R is the proper transform of the original $\mathbf{P}^1(x)$ ruling over the s -line $t = 0$. The numbers indicate the bidegrees of the normal bundles of various rational curves. Taking double cover of the blown-up threefold yields the configuration represented in fig. 18.b. The

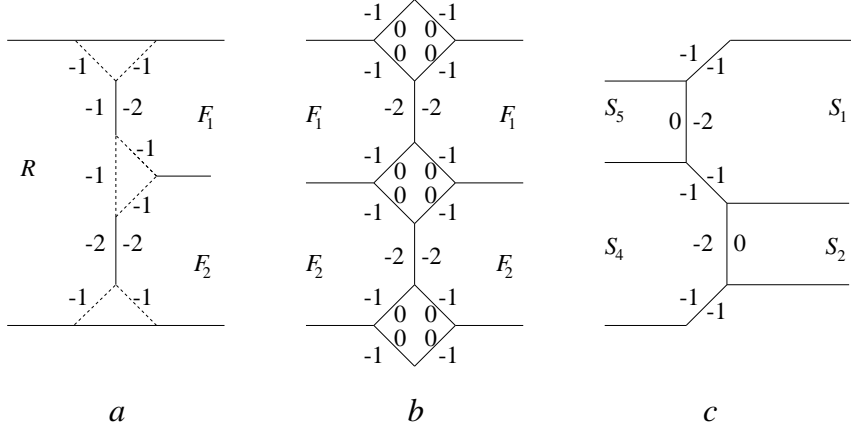


Fig. 18: Construction of the smooth threefold model. The configuration *b* represents the double cover of *a*.

surface R is no longer explicitly represented there. Note that the exceptional \mathbf{P}^2 components are covered by \mathbf{F}_0 surfaces. Finally, a smooth threefold model with one-dimensional fibers can be obtained by contracting the exceptional \mathbf{F}_0 surfaces in any direction. A possible contraction and the resulting smooth model are described in fig. 18c. It can be easily checked that this is precisely the E_6 degeneration of section three. For clarity, we have identified the exceptional ruled surfaces. Different contractions of the \mathbf{F}_0 surfaces result in different geometric phases as in section three.

Appendix C. Resolution of the E_7 Weierstrass Model

We consider a singular Weierstrass model with

$$\begin{aligned} f(z_1, z_2) &= z_1^3 f_{8+n}(z_2) \\ g(z_1, z_2) &= z_1^5 g_{12+n}(z_2). \end{aligned} \tag{C.1}$$

The discriminant of the elliptic fibration is given by

$$\Delta = z_1^9 (4f_{8+n}^3(z_2) + O(z_1)). \tag{C.2}$$

Taking into account the vanishing orders of f, g, Δ [16], there is a line $z_1 = 0$ of III^* fibers colliding a second line of I_1 singularities at the zeroes of f_{8+n} . Based on the dual heterotic model, there should each zero of f_{8+n} should correspond to a half-hypermultiplet in the **56** representation.

The smooth flat model can be constructed as follows. The singularity can be written locally near a simple zero of f_{8+n} as

$$y^2 = x^3 + s^3tx + s^5. \quad (\text{C.3})$$

We have

$$f = s^3t, \quad g = s^5, \quad \Delta = s^9(4t^3 + 27s). \quad (\text{C.4})$$

The vanishing degrees of (f, g, Δ) along $s = 0$ are $(3, 5, 9)$ characterizing a III^* fiber. The vanishing degrees over $4t^3 + 27s = 0$ are $(0, 0, 1)$, therefore we obtain a line of I_1 fibers colliding $s = 0$ at $s = t = 0$. At the collision locus, the vanishing degrees jump to $(4, 5, 10)$ signaling a II^* fiber. This jump is expected to give rise to a half-hypermultiplet in the **56** representation. We explicitly show that this is the case by constructing the corresponding smooth model.

The elliptic fibration can be represented as a double cover of a $\mathbf{P}^1(x)$ bundle over the (s, t) plane branched over the surface B

$$x^3 + s^3tx + s^5 = 0. \quad (\text{C.5})$$

As in the previous case, the problem can be reduced to the elliptic surface case by taking slices through points in the discriminant. For fixed generic $t \neq 0$ the singularity is of analytic type $x^3 + s^3x$ corresponding to a III^* fiber over the t -line. For $t = 0$, the singularity is of analytic type $x^3 + s^5$ which corresponds to a II^* fiber. The resolution follows the steps outlined in appendix B. First, we successively blow-up the line $x = s = 0$ until the generic III^* fiber is resolved. This process is represented in fig. 19.

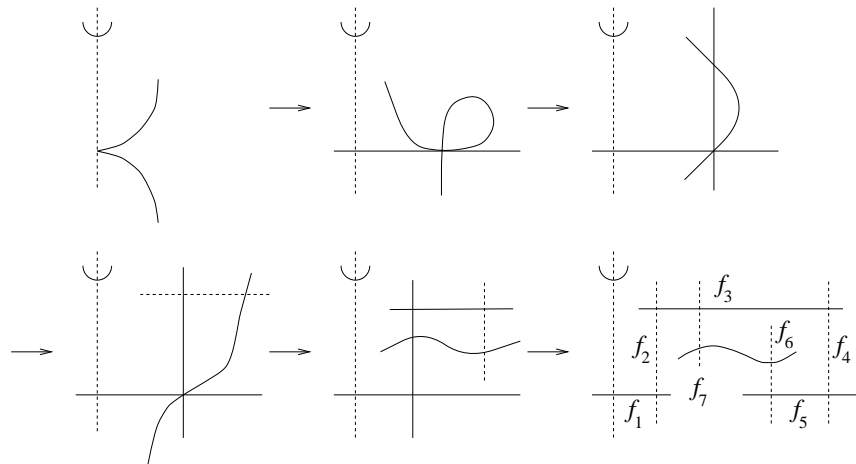


Fig. 19: Resolution of the generic III^* fiber.

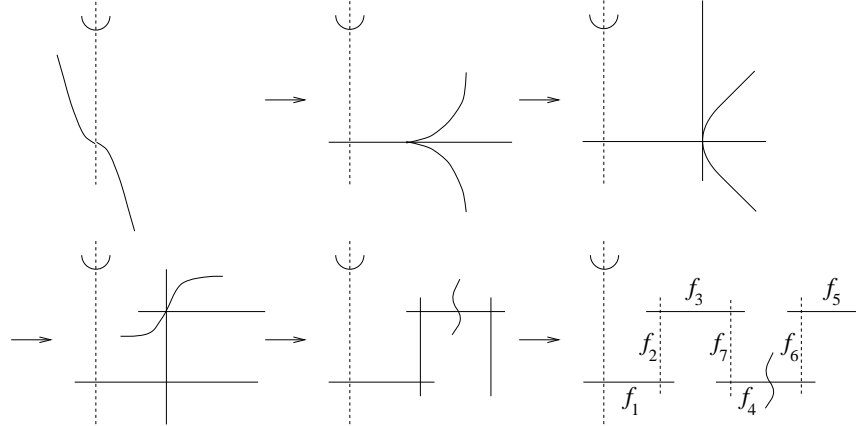


Fig. 20: Partial resolution of the II^* fiber over the collision locus. The limitations of two dimensional drawing prevent a correct representation of the original singular branch locus.

The sequence of blow-ups leads to a partial resolution of the II^* fiber over the collision locus as in fig. 20. Note that the branch locus intersects itself over the collision locus. However, the branch surface is of analytic type $uv = w$ near the intersection point. As this is smooth, the double cover is also smooth and no further blow-ups are necessary. Taking into account the structure of the singular fiber over the collision point, it follows that this is precisely the first E_7 degeneration introduced in section 4.

References

- [1] N. Seiberg, “Five-Dimensional SUSY Field Theories, Nontrivial Fixed Points and String Dynamics”, *Nucl. Phys.* **B483** (1997) 229, hep-th/9608111.
- [2] N. Seiberg and D. R. Morrison, “Extremal Transitions and Five-Dimensional Supersymmetric Field Theories”, *Nucl. Phys.* **B483** (1997) 229, hep-th/9609070.
- [3] M. R. Douglas, S. Katz and C. Vafa, “Small Instantons, del Pezzo Surfaces and Type I’ Theory”, *Nucl. Phys.* **B497** (1997) 155, hep-th/9609071
- [4] K. Intriligator, D.R. Morrison and N. Seiberg, “Five-Dimensional Supersymmetric Gauge Theories and Degenerations of Calabi-Yau Spaces”, *Nucl. Phys.* **B497** (1997) 56, hep-th/9702198.
- [5] N. Nekrasov, “Five Dimensional Gauge Theories and Relativistic Integrable Systems”, hep-th/9609219.
- [6] O. Aharony and A. Hanany, “Branes, Superpotentials and Superconformal Fixed Points”, *Nucl. Phys.* **B504** (1997) 239, hep-th/9704170.
- [7] O. Aharony, A. Hanany and B. Kol, “Webs of (p,q) 5-branes, Five Dimensional Field Theories and Grid Diagrams”, hep-th/9710116.
- [8] N.C. Leung and C. Vafa, “Branes and Toric Geometry”, hep-th/9711013.
- [9] S. Katz, A. Klemm and C. Vafa, “Geometric Engineering of Quantum Field Theories”, *Nucl. Phys.* **B497** (1997) 173, hep-th/9609239.
- [10] S. Katz and C. Vafa, “Geometric Engineering of N=1 Quantum Field Theories”, *Nucl. Phys.* **B497** (1997) 196, hep-th/9611090.
- [11] M. Bershadsky, A. Johansen, T. Pantev, V. Sadov and C. Vafa, “F-theory, Geometric Engineering and N=1 Dualities”, *Nucl. Phys.* **B505** (1997) 153, hep-th/9612052.
- [12] S. Katz, P. Mayr and C. Vafa, “Mirror symmetry and Exact Solution of 4D N=2 Gauge Theories I”, hep-th/9706110.
- [13] S. Katz, D.R. Morrison and M.R. Plesser, “Enhanced Gauge Symmetry in Type II String Theory”, *Nucl. Phys.* **B477** (1996) 105, hep-th/9601108.
- [14] W. Nahm, “Supersymmetries and Their Representations”, *Nucl. Phys.* **B135** (1978) 149.
- [15] D.R. Morrison and C. Vafa, “Compactifications of F-Theory on Calabi–Yau Threefolds – I”, *Nucl. Phys.* **B473** (1996) 74, hep-th/9602114; “Compactifications of F-Theory on Calabi–Yau Threefolds – II”, *Nucl. Phys.* **B476** (1996) 437 hep-th/9603161.
- [16] M. Bershadsky, K. Intriligator, S. Kachru, D.R. Morrison, V. Sadov and C. Vafa, “Geometric Singularities and Enhanced Gauge Symmetries”, *Nucl. Phys.* **B481** (1996) 215, hep-th/96050200.
- [17] R. Miranda, “Smooth Models for Elliptic Threefolds”, in R. Friedman and D.R. Morrison, editors, “The Birational Geometry of Degenerations”, Birkhauser, 1983.

- [18] P.S. Aspinwall and M. Gross, “The $SO(32)$ Heterotic String on a K3 Surface”, Phys. Lett. **B387** (1996) 735, hep-th/9605131.
- [19] P.S. Aspinwall, “Point-Like Instantons and the $Spin(32)/Z_2$ Heterotic String”, Nucl. Phys. **B496** (1997) 149, hep-th/9612108.
- [20] P.S. Aspinwall, D.R. Morrison, “Point-like Instantons on K3 Orbifolds”, Nucl. Phys. **B503** (1997) 533, hep-th/9705104.
- [21] R. Hartshorne, “Algebraic Geometry”, Graduate Texts in Mathematics, Springer-Verlag (1993).
- [22] M. Demazure, in “Séminaire sur les Singularités des Surfaces”, (M. Demazure, H. Pinkham and B. Teissier - eds.), Lecture Notes in Mathematics **777** Springer-Verlag, 1980, p. 24.
- [23] M. Reid, “Chapters on Algebraic Surfaces”, alg-geom/9602006.